Energetic Particle Interaction with MHD Instabilities

傅国勇

浙江大学聚变理论与模拟中心

Outline

- Introduction to Energetic Particle (EP) Physics
- Hybrid model
- Quadratic form
- EP interaction with MHD modes
  - Internal kink mode/fishbone
  - Ballooning modes
  - Tearing mode
  - Resistive Wall Mode (RWM)
- Summary

Energetic Particle Sources

- Typical fusion plasmas have density n_{th}~ $10^{20}m^{-3}$and T_{th}~10kev

- Typical energetic particle energy E_h~100kev >> T_{th} .

- In current tokamak devices, energetic particles are usually introduced by neutral beam injection (NBI heating) or by Radio Frequency wave heating (RF heating).

- In a fusion reactor, energetic alpha particles are produced by fusion reactions:

$$D + T \rightarrow \alpha\ (3.5Mev) + n\ (14Mev)$$

- Energetic particles 高能量粒子, fast particles/hot particles 快粒子, beam ions 束离子

Energetic particle physics is one of key research areas in fusion plasmas

Fusion plasma research topics:

- Equilibrium
- MHD stability
- Transport
- Heating and current drive
- Edge physics
- Plasma wall interaction

Energetic Particle Physics (effects on equilibrium, MHD stability, Alfven Eigenmodes (AE), transport etc)

Roles of energetic particles in fusion plasmas

- Heat plasmas via Coulomb collisions, current drive
- Influence MHD stability
- Destabilize Alfven waves via wave-particle resonances (Alfven eigenmodes and Energetic Particle Mode)
- Energetic particle redistribution/losses due to 3D perturbations can degrade plasma heating, and damage reactor wall (e.g., ripple, MHD modes etc)
- Energetic particles can affect thermal plasmas via their effects on equilibrium, stability and transport

Single Particle Confinement

•Constants of motion: energy, magnetic moment and toroidal angular momentum.

•For an axi-symmetric torus, particles are confined as long as orbit width is not too large. (conservation of toroidal angular momentum.)

•Toroidal field ripple (due to discrete coils) or other external 3D perturbations (e.g., RMP) can induce anomalous transport of energetic particles.

•Symmetry-breaking MHD modes (sawtooth, NTM etc) can also cause energetic particle anomalous transport.

Shear Alfven spectrum and continuum damping

- Shear Alfven wave dispersion relation
- Continuum spectrum $$\omega^2 = k_\parallel^2 V_A^2 = \frac{1}{R^2}\left(n - \frac{m}{q(r)}\right)^2 \frac{B^2}{\rho(r)}$$
- Driven perturbation at ω is resonantly absorbed at

$\omega = \omega_A(r)$ → continuum damping

Continuum spectrum, gaps, Alfven eigenmodes

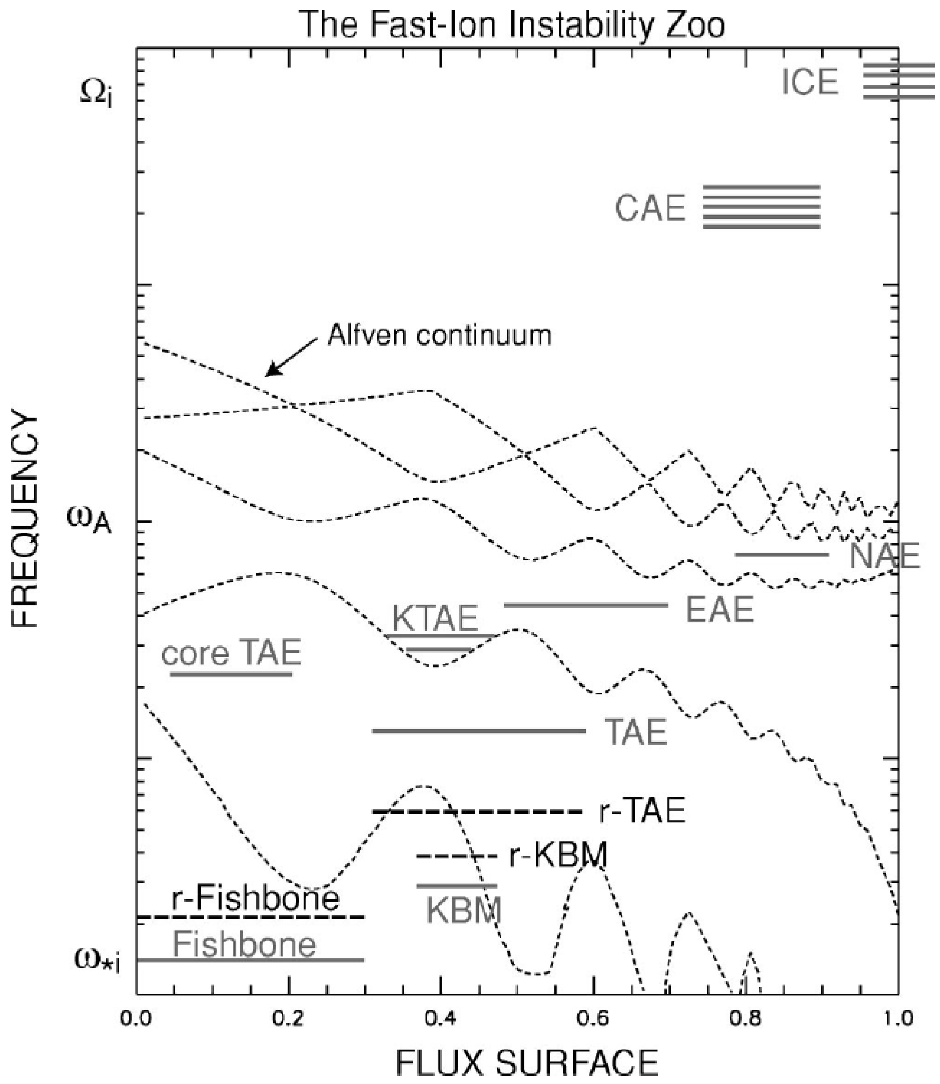

Coupling of m and m+k modes breaks degeneracy of Alfven continuum :

$$\left| n - \frac{m}{q} \right| = \left| n - \frac{m+k}{q} \right| \; at$$

$$q = \frac{2m+k}{2n}$$

k=1 coupling by toroidicity
k=2 coupling by elongation
k=3 coupling triangularity.

Discrete Alfven Eigenmodes versus Energetic Particle Modes

- Discrete Alfven Eigenmodes (AE):
  Mode frequencies located outside Alfven continuum (e.g., inside gaps);
  Modes exist in the MHD limit;
  energetic particle effects are often perturbative.

- Energetic Particle Modes (EPM):
  Mode frequencies located inside Alfven continuum and determined by energetic particle dynamics;
  Energetic effects are non-perturbative;
  Requires sufficient energetic particle drive to overcome continuum damping.

Example of Discrete AE: Toroidal Alfven Eigenmode (TAE)

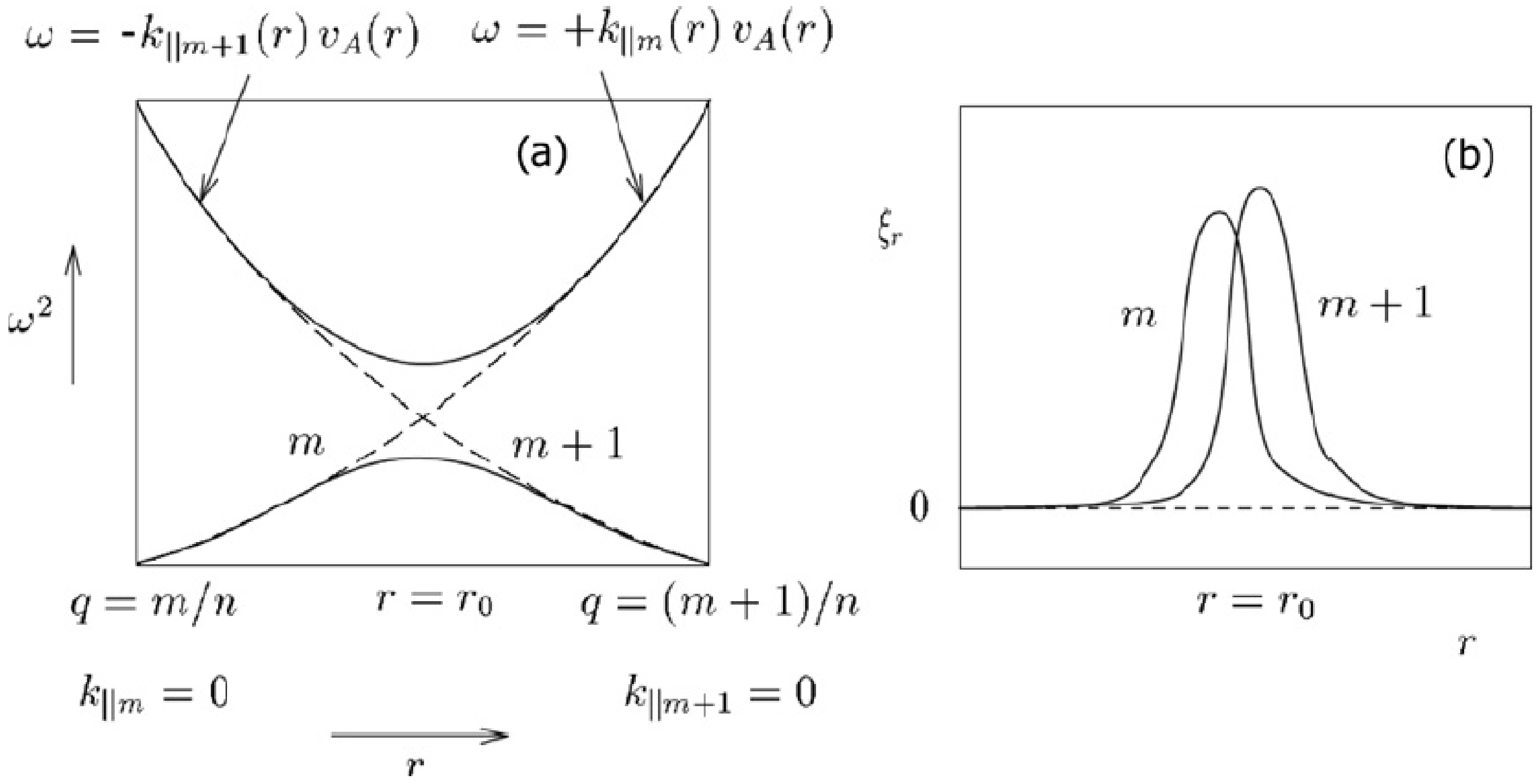

TAE mode frequencies are located inside the toroidcity-induced Alfven gaps; TAE modes peak at the gaps with two dominating poloidal harmonics.

C.Z. Cheng, L. Chen and M.S. Chance 1985, *Ann. Phys. (N.Y.)* **161**, 21

Destabilize shear Alfven waves via wave-particle resonance

- Destabilization mechanism (universal drive)

Wave particle resonance at $\omega = k_{\|} v_{\|}$
Particles lose/gain energy going outward/inward. As a result, particles lose energy to waves due to density gradient (free energy!)

$$\frac{dP_\phi}{dt} = -\frac{n}{\omega}\frac{dE}{dt}$$

Energetic particle drive $\frac{\gamma}{\omega} \propto \beta_h[-\frac{n}{\omega}\frac{E_h df}{f dP_\phi} + \frac{E_h df}{f dE}]$

Spatial gradient drive

Landau damping
Due to velocity space gradient

Example of EPM: fishbone instability

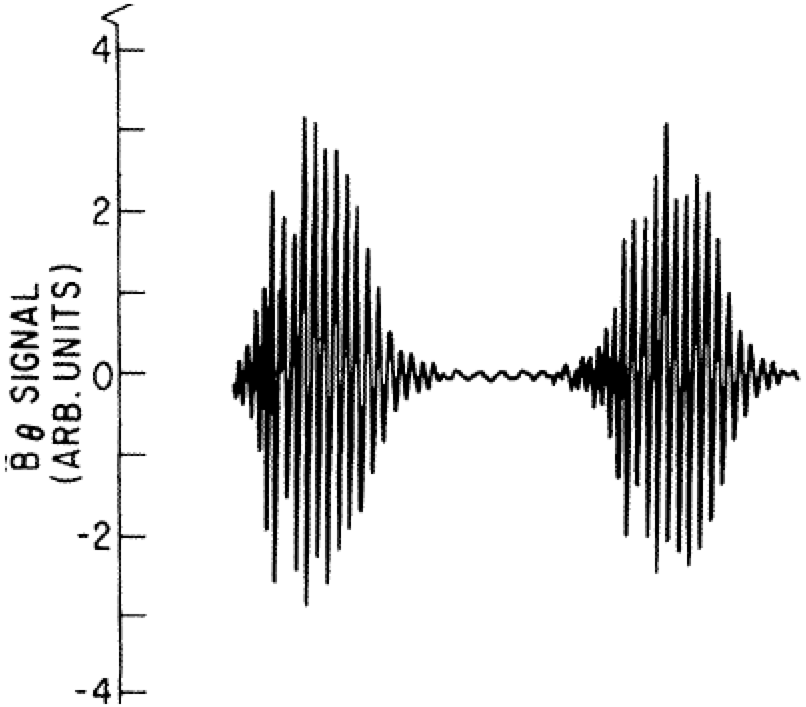

Mode structure is of (m,n)=(1,1) internal kink;

Mode is induced by energetic trapped particles;

Mode frequency is comparable to trapped particles' precessional drift frequency.

Mode frequency is inside Alfven continuum.

K. McGuire, R. Goldston, M. Bell, *et al.* 1983, *Phys. Rev. Lett.* **50**, 891
L. Chen, R.B. White and M.N. Rosenbluth 1984, *Phys. Rev. Lett.* **52**, 1122

Outline

- Introduction to Energetic Particle (EP) Physics
- Hybrid model
- Quadratic form
- EP interaction with MHD modes
  - Internal kink mode/fishbone
  - Ballooning modes
  - Tearing mode
  - Resistive Wall Mode (RWM)
- Summary

Kinetic/MHD Hybrid Model

$$\rho \frac{d\mathbf{v}}{dt} = -\nabla P - \nabla \cdot \mathbf{P}_h + \mathbf{J} \times \mathbf{B}$$

$$\mathbf{J} = \nabla \times \mathbf{B}, \quad \frac{\partial \mathbf{B}}{\partial t} = -\nabla \times \mathbf{E}$$

$$\mathbf{E} + \mathbf{v} \times \mathbf{B} = \eta \mathbf{J}$$

$$\frac{\partial \rho}{\partial t} + \nabla \cdot (\rho \mathbf{v}) = 0$$

$$\frac{dp}{dt} = -\gamma p \nabla \cdot \mathbf{v} + \rho \nabla \cdot \overleftrightarrow{\kappa} \cdot \nabla \frac{p}{\rho}$$

CGL form:

$$\mathbf{P}_h = P_\perp \mathbf{I} + (P_\parallel - P_\perp)\mathbf{b}\mathbf{b}$$

Guiding center distribution:

$$F = F(\mathbf{X}, v_\parallel, \mu) = \sum_i \delta(\mathbf{X} - \mathbf{X}_i)\delta(v_\parallel - v_{\parallel,i})\delta(\mu - \mu_i)$$

Gyrokinetic or drift kinetic equations:

$$\frac{d\mathbf{X}}{dt} = \frac{1}{B^{\star\star}}[v_\parallel \mathbf{B}^\star - \mathbf{b}_0 \times (\langle \mathbf{E} \rangle - \frac{1}{e}\mu \nabla (B_0 + \langle \delta B \rangle))]$$

$$m \frac{dv_\parallel}{dt} = \frac{e}{B^{\star\star}} \mathbf{B}^\star \cdot [\langle \mathbf{E} \rangle - \frac{1}{e}\mu \nabla (B_0 + \langle \delta B \rangle)]$$

$$\mathbf{B}^\star = \mathbf{B}_0 + \langle \delta \mathbf{B} \rangle + \frac{m v_\parallel}{q} \nabla \times \mathbf{b}_0, \quad B^{\star\star} = \mathbf{B}^\star \cdot \mathbf{b}_0$$

G. Y. Fu, et al., Phys. Plasmas 13, 052517 (2006).

Outline

- Introduction to Energetic Particle (EP) Physics
- Hybrid model
- Quadratic form
- EP interaction with MHD modes
  - Internal kink mode/fishbone
  - Ballooning modes
  - Tearing mode
  - Resistive Wall Mode (RWM)
- Summary

Quadratic form

$$\rho \frac{\partial \vec{V}}{\partial t} = -\nabla \delta P_b - \nabla \cdot \delta \overleftrightarrow{P}_h + \delta \vec{J} \times \vec{B} + \vec{J} \times \delta \vec{B}$$

$$\delta P_h = \delta P_\perp \overleftrightarrow{I} + (\delta P_\parallel - \delta P_\perp) \vec{b}\vec{b} + (P_\parallel - P_\perp)(\delta \vec{b}\, \vec{b} + \vec{b}\, \delta \vec{b})$$

$$\frac{\partial \vec{V}}{\partial t} = -\omega^2 \vec{\xi}$$

$$\omega^2 \delta K = \delta W_f + \delta W_k$$

where $\delta K = \frac{1}{2} \int d^3x\, \rho |\vec{\xi}|^2$

$$\delta W_f = \frac{1}{2} \int d^3x\, \vec{\xi}^* \cdot \left(\nabla \delta P_b + \nabla \cdot \delta \overleftrightarrow{P}_{h,f} - \delta \vec{J} \times \vec{B} - \vec{J} \times \delta B \right)$$

$$\delta W_k = \frac{1}{2} \int d^3x\, \vec{\xi}^* \cdot \nabla \cdot \delta \overleftrightarrow{P}_{h,k}$$

G.Y. Fu et al. Phys. Fluids B5, 4040 (1993)

Drift-kinetic Equation for Energetic Particle Response

$$\delta P_{\parallel} = \int d^3v \, m v_{\parallel}^2 \, \delta f$$

$$\delta P_{\perp} = \int d^3v \, \frac{1}{2} m v_{\perp}^2 \, \delta f$$

$$\delta f = -\vec{\xi}_{\perp} \cdot \nabla f_h + g$$

$$\left(\frac{\partial}{\partial t} + v_{\parallel} \vec{b} \cdot \nabla + \vec{v}_d \cdot \nabla \right) g = 2 i E \frac{\partial f_h}{\partial E} (\omega - \omega_*) G$$

where $\omega_* = n \dfrac{\partial f_h}{\partial P_\varphi} \Big/ \dfrac{\partial f_h}{\partial E}$, $P_\varphi = e\psi + m v_\varphi R$

$$G \equiv \frac{e}{2E} \left(\frac{i}{\omega} \vec{v}_d \cdot \delta \vec{E} \right)$$

$$\delta W_k = - \int d^3x \int d^3v \, E \, G^* g$$

Quadratic form

$$\delta W_k = \frac{8\pi^2}{m^2 B_0} \sum_{p,\sigma} \int d\psi \, dE \, d\Lambda \, E^3 \frac{\partial f_h}{\partial E} (\omega - \omega_*) \tau_b \frac{|\hat{G}_p|^2}{p\omega_\theta - n\omega_\varphi - \omega}$$

where $G \equiv \hat{G}(\psi, \theta) e^{-i(n\varphi + \omega t)}$

$$\varphi(t) \equiv \omega_\varphi t + \hat{\varphi}(t) \qquad \text{(particle orbit)}$$

$$\hat{G}_p = \frac{1}{\tau_b} \oint \hat{G}(\psi, \theta) e^{-i(p\omega_\theta t + n\hat{\varphi}(t))} dt$$

τ_b is the period of particle orbit

G.Y. Fu et al. Phys. Fluids B5, 4040 (1993)

Outline

- Introduction to Energetic Particle (EP) Physics
- Hybrid model
- Quadratic form
- EP interaction with MHD modes
  - Internal kink mode/fishbone
  - Ballooning modes
  - Tearing mode
  - Resistive Wall Mode (RWM)
- Summary

EP interaction with internal kink mode

- Stabilization of internal kink by trapped energetic particles;
- Excitation of fishbone by trapped energetic particles;
- Excitation of fishbone by passing particles
- Hybrid simulations of energetic particle interaction with internal kink mode

Stabilization of internal kink by trapped energetic particles

For trapped particles and $p = 0$

$$\delta W_k = -\frac{8\pi^2}{m^2 B_0} \int d\psi \, d\bar{E} \, d\Lambda \, E^3 \frac{\partial f_h}{\partial E} \tau_b \frac{(\omega - \omega_*)}{\omega - \omega_d} |\hat{G}_0|^2$$

where $\omega_d = -n\omega_\varphi$, $\hat{G}_0 \approx \langle \hat{G} \rangle$

for $\omega \ll \omega_d$, $\omega \ll \omega_*$

$$\frac{\omega - \omega_*}{\omega - \omega_d} \Longrightarrow \frac{\omega_*}{\omega_d} > 0 \Rightarrow \delta W_k > 0$$

$\Rightarrow$ stabilizing !

Experimental observation of fishbone instability in PDX

VOLUME 50, NUMBER 12 PHYSICAL REVIEW LETTERS 21 MARCH 1983

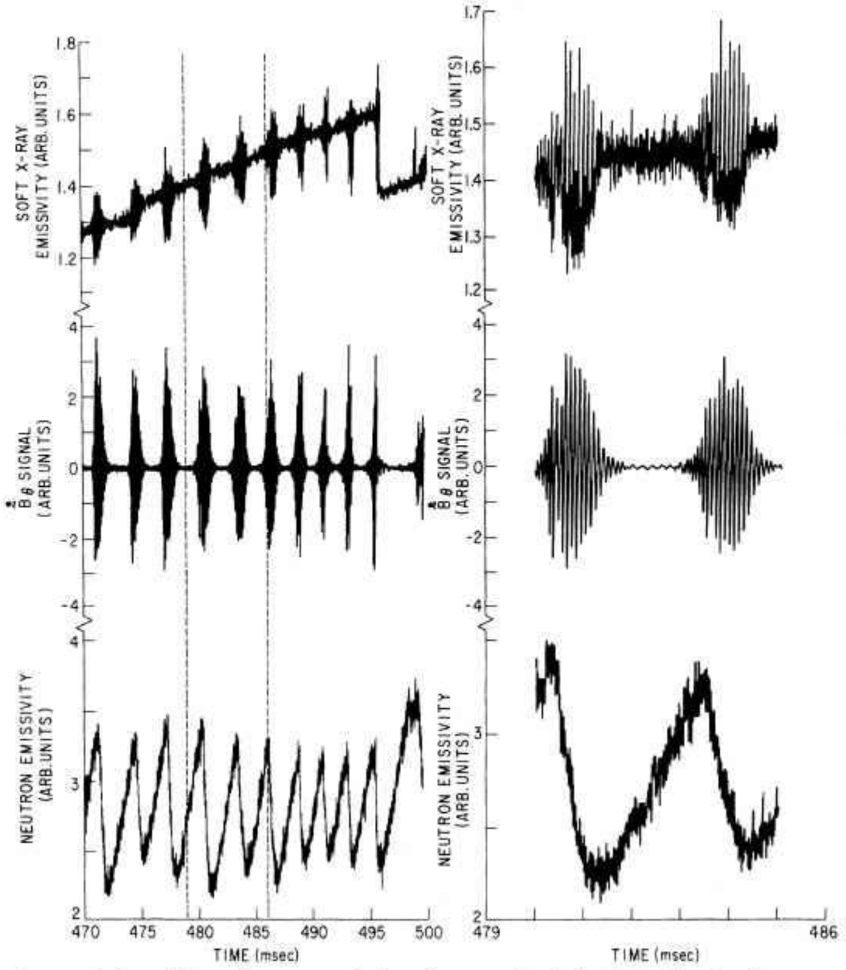

FIG. 1. The time evolution of the soft–x-ray emission along a central chord, the $\dot{B}_\theta$ signal from a coil near the outer wall of the vacuum vessel, and the fast neutron flux. Expansion of the data near two "fishbones" is also shown.

K. McGuire, R. Goldston, M. Bell, et al. 1983, Phys. Rev. Lett. 50, 891

Brief history of fishbone

- 1983: discovery of beam-driven fishbone in PDX (McGuire PRL 1983);
- 1984: theory of fishbone driven by energetic trapped particle via precessional resonance, (Chen PRL 1984);
  - $\omega \sim \omega_d$
- 1986: theory of fishbone driven by energetic trapped particles (Coppi PRL 1986);
  - $\omega \sim \omega_*$
- 1986: discovery of fishbone driven by passing beam ions in PBX (Heidbrink PRL 1986);
- 1993: theory of fishbone driven by passing energetic ions (Betti PRL 1993);
  - $\omega \sim \omega_*$
- 2001: theory of fishbone driven by passing energetic ions (Wang PRL 2001)
  - $\omega \sim \omega_\phi$
- 2019: theory of low-frequency fishbone driven by passing energetic ions (Yu NF 2019)
  - $\omega \sim \omega_\phi - \omega_\theta$

Theory of Fishbone Instabilities

$$\omega = n\omega_\phi + p\omega_\theta$$

	Trapped particle	Passing particle
EPM	p=0, $\omega \simeq \omega_{dh}$ L. Chen PRL 1984	p=0, $\omega = \omega_\phi$ High frequency , S.J. Wang, PRL 2001.
ω_{*i} Mode	p=0, $\omega = \omega_{*i}$ B. Coppi, PRL, 1986	p=-1, $\omega = \omega_{*i} \simeq \omega_\phi - \omega_\theta$ R. Betti PRL 1993

Fishbone dispersion relation (trapped particles)

$$-i\omega/\tilde{\omega}_A + \delta\hat{W}_f + \delta\hat{W}_k = 0.$$

$$\delta W_k = -2^{9/2}\pi^3 m_h \int RBr\,dr \int_{B_{\max}^{-1}}^{B_{\min}^{-1}} d\alpha \int_\theta^\infty dE\, E^{5/2} K_b \bar{J}^* \frac{Q}{\omega - \bar{\omega}_{dh}} \bar{J};$$

$$-i\Omega(\bar{\omega}_{dm}/\tilde{\omega}_A) + \delta\hat{W}_{fc} + \langle\beta_{h,t}\hat{I}_0\rangle\,\Omega\,\ln(1-1/\Omega) = 0$$

$$\Omega = \frac{\omega}{\bar{\omega}_{dm}}$$

L. Chen, R.B. White and M.N. Rosenbluth 1984, *Phys. Rev. Lett.* **52**, 1122

Fishbone dispersion relation (trapped particles)

$$-i\Omega(\bar{\omega}_{dm}/\tilde{\omega}_A) + \delta\hat{W}_{fc} + \langle\beta_{h,t}\hat{I}_0\rangle\,\Omega\ln(1 - 1/\Omega) = 0$$

$$\Omega = \frac{\omega}{\bar{\omega}_{dm}}$$

Consider $\delta\hat{W}_{fc} = 0$

At marginal stability $\langle\beta_{h,t}\hat{I}_0\rangle = \frac{\bar{\omega}_{dm}}{\pi\tilde{\omega}_A}$

$\Omega = \frac{1}{2}$ or $\omega_r = \frac{1}{2}\bar{\omega}_{dm}$

$\Rightarrow$ growth rate $\gamma \approx \tilde{\omega}_A \frac{\pi^2}{4}\left(\langle\beta_{h,t}\hat{I}_0\rangle - \langle\beta_{h,t}\hat{I}_0\rangle_{crit}\right)$

Simulation of Fishbone Instability

G.Y. Fu et al., Phys. Plasmas, 2006

Model used in M3D-K

$$\rho\frac{d\mathbf{v}}{dt} = -\nabla P - \nabla\cdot\mathbf{P}_h + \mathbf{J}\times\mathbf{B}$$

$$\mathbf{J} = \nabla\times\mathbf{B}, \quad \frac{\partial\mathbf{B}}{\partial t} = -\nabla\times\mathbf{E}$$

$$\mathbf{E} + \mathbf{v}\times\mathbf{B} = \eta\mathbf{J}$$

$$\frac{\partial\rho}{\partial t} + \nabla\cdot(\rho\mathbf{v}) = 0$$

$$\frac{dp}{dt} = -\gamma p\nabla\cdot\mathbf{v} + \rho\nabla\cdot\overleftrightarrow{\kappa}\cdot\nabla\frac{p}{\rho}$$

CGL form:

$$\mathbf{P}_h = P_\perp\mathbf{I} + (P_\parallel - P_\perp)\mathbf{bb}$$

Guiding center distribution:

$$F = F(\mathbf{X}, v_\parallel, \mu) = \sum_i \delta(\mathbf{X}-\mathbf{X}_i)\delta(v_\parallel - v_{\parallel,i})\delta(\mu-\mu_i)$$

Gyrokinetic or drift kinetic equations:

$$\frac{d\mathbf{X}}{dt} = \frac{1}{B^{\star\star}}[v_\parallel\mathbf{B}^\star - \mathbf{b}_0\times(\langle\mathbf{E}\rangle - \frac{1}{e}\mu\nabla(B_0 + \langle\delta B\rangle))]$$

$$m\frac{dv_\parallel}{dt} = \frac{e}{B^{\star\star}}\mathbf{B}^\star\cdot[\langle\mathbf{E}\rangle - \frac{1}{e}\mu\nabla(B_0+\langle\delta B\rangle)]$$

$$\mathbf{B}^\star = \mathbf{B}_0 + \langle\delta\mathbf{B}\rangle + \frac{mv_\parallel}{q}\nabla\times\mathbf{b}_0, \quad B^{\star\star} = \mathbf{B}^\star\cdot\mathbf{b}_0$$

G. Y. Fu, et al., Phys. Plasmas 13, 052517 (2006).

Excitation of Fishbone at high β_h

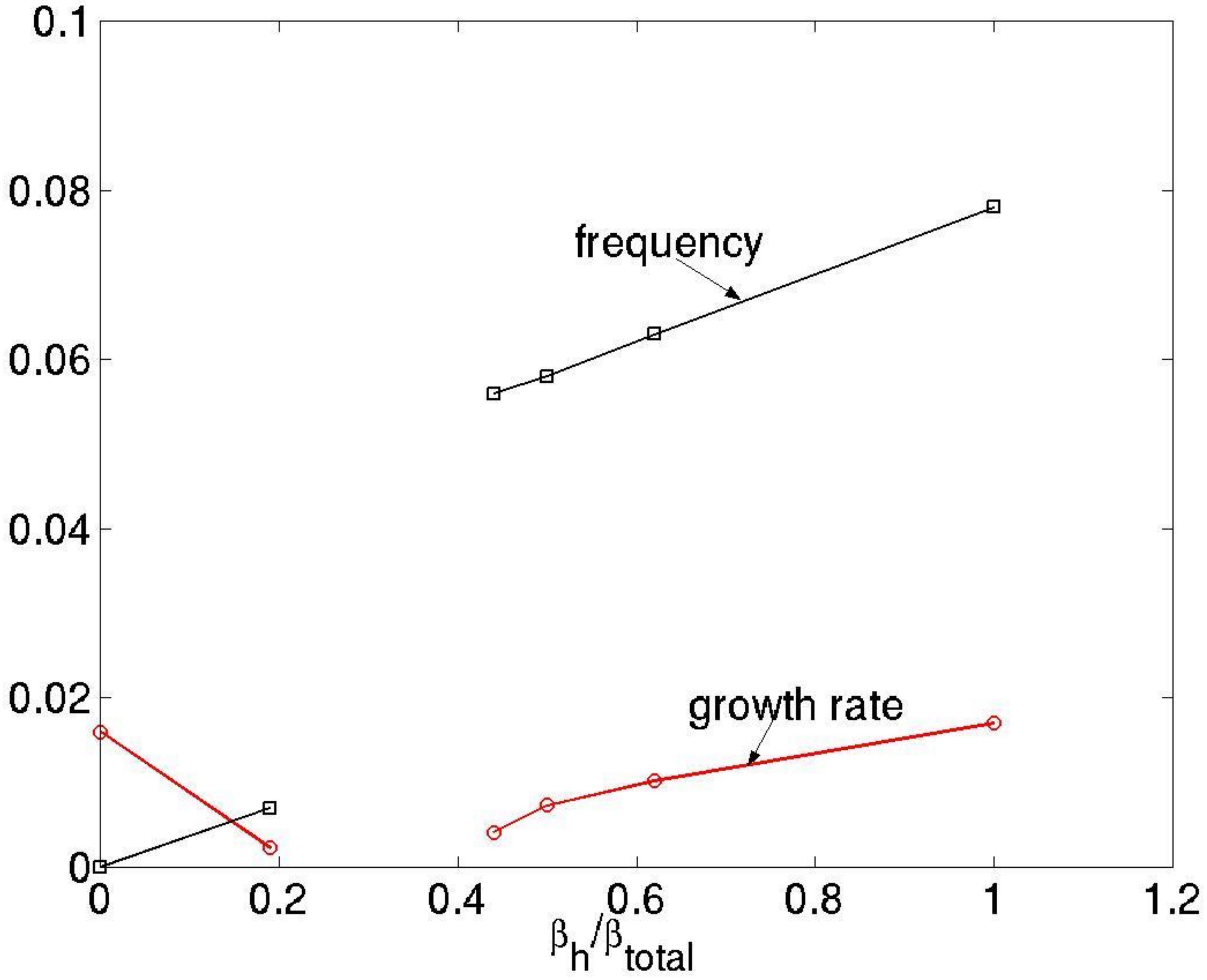

Mode Structure: Ideal Kink v.s. Fishbone

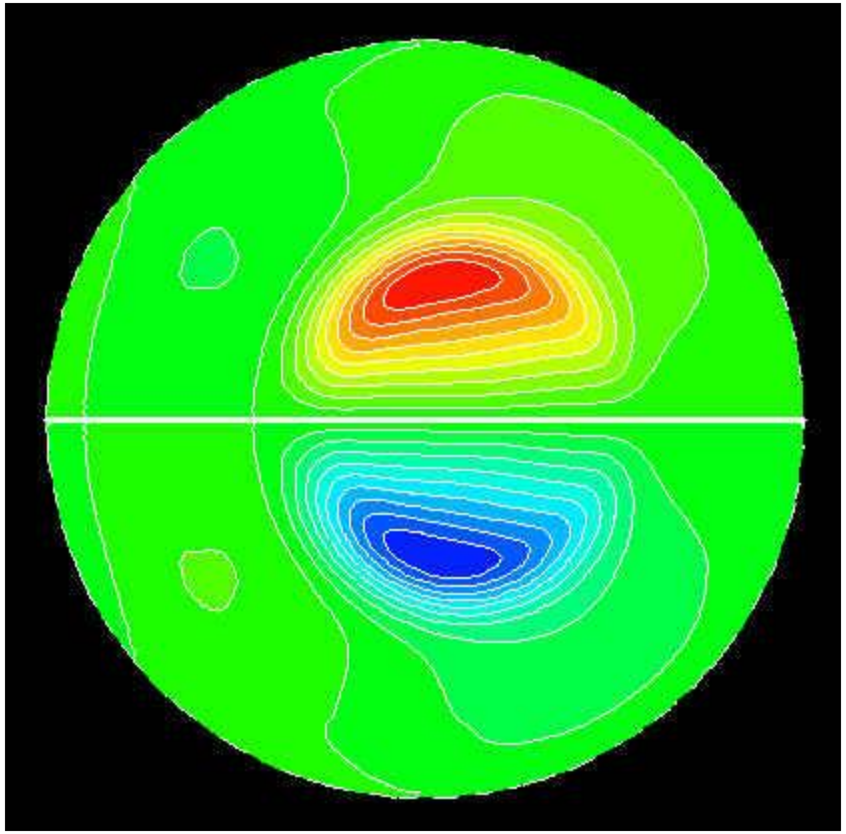

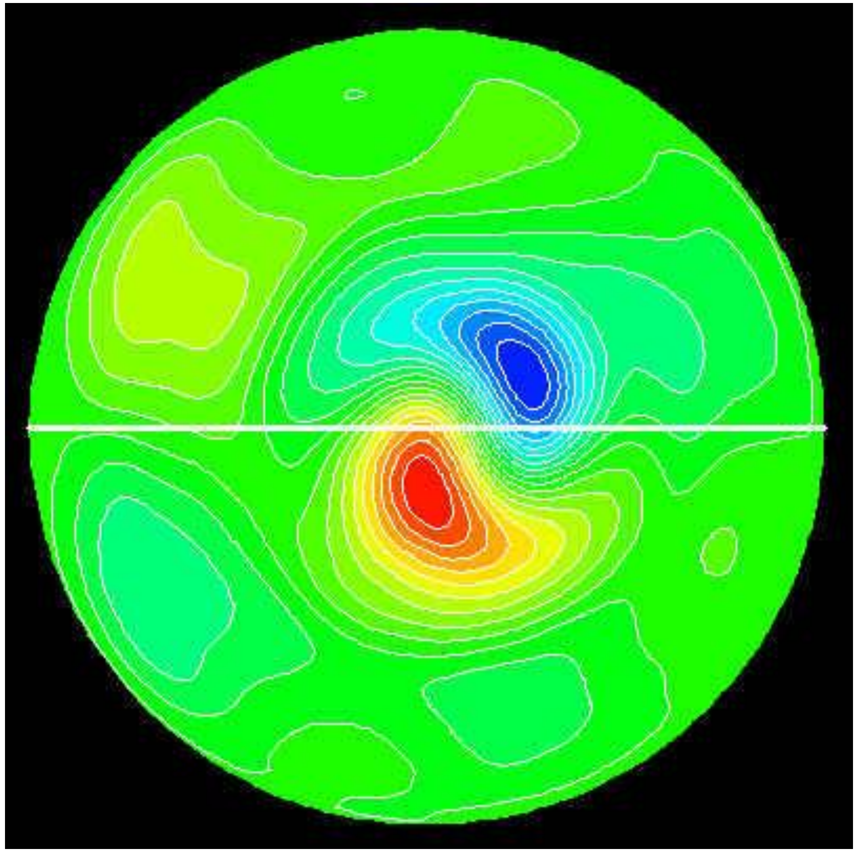

Nonlinear evolution of mode structure and mode amplitude

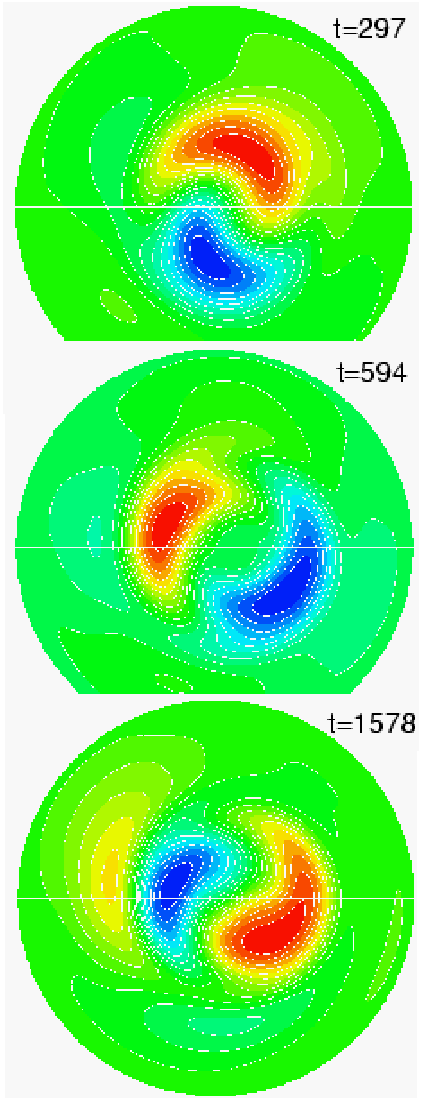

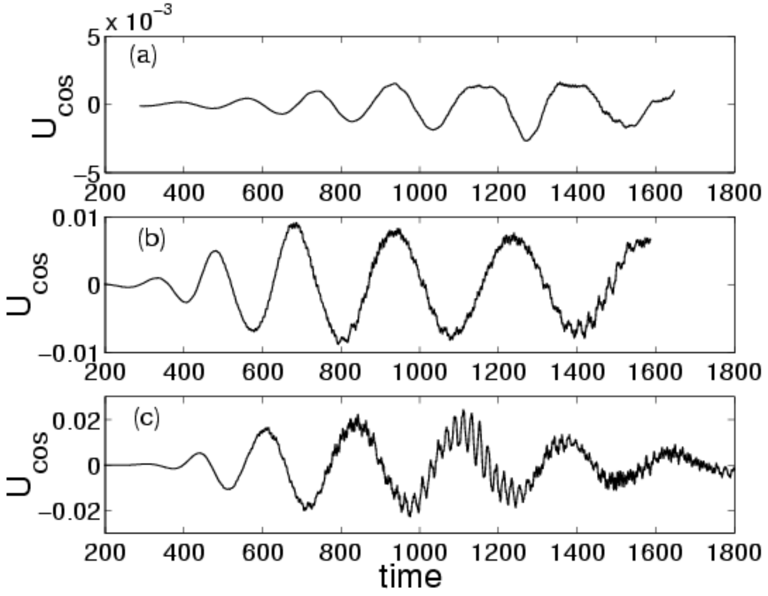

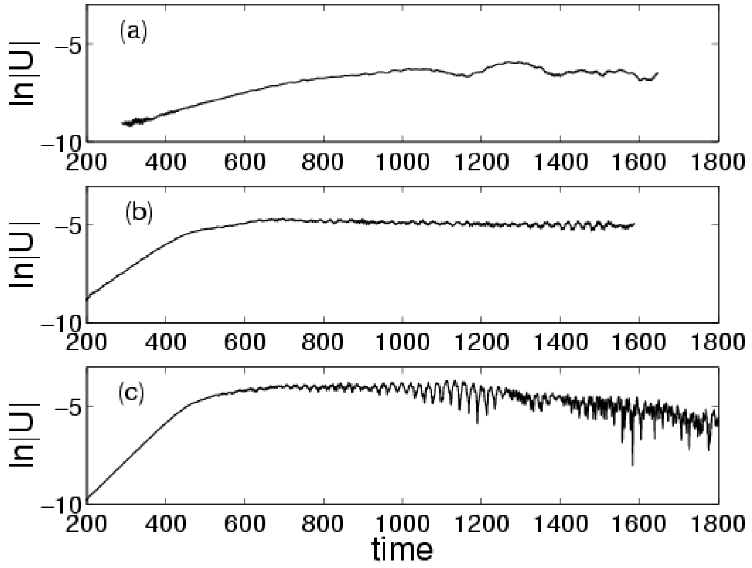

Simulation of fishbone shows distribution fattening and strong frequency chirping

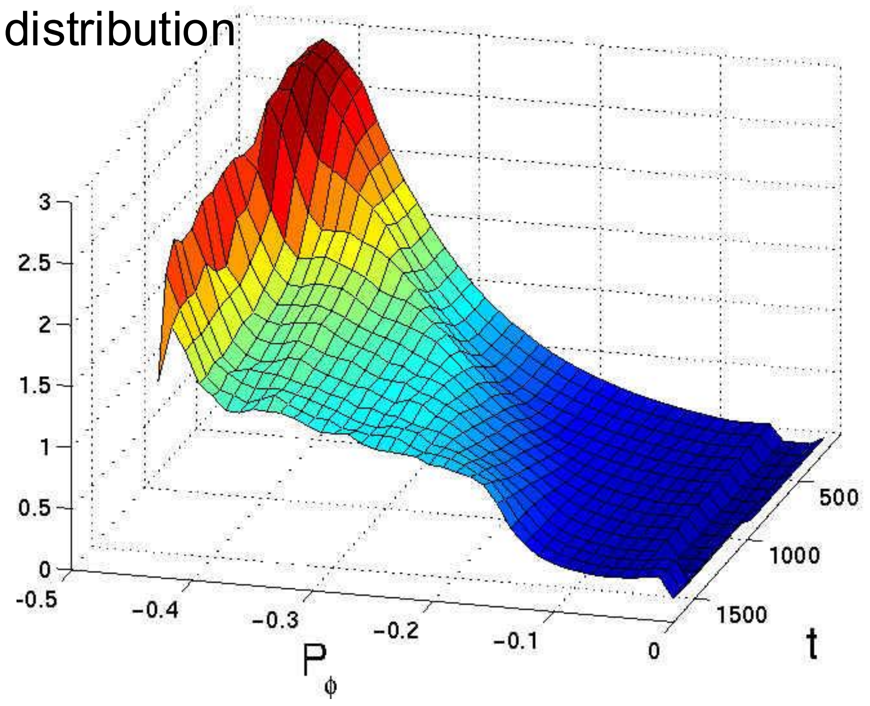

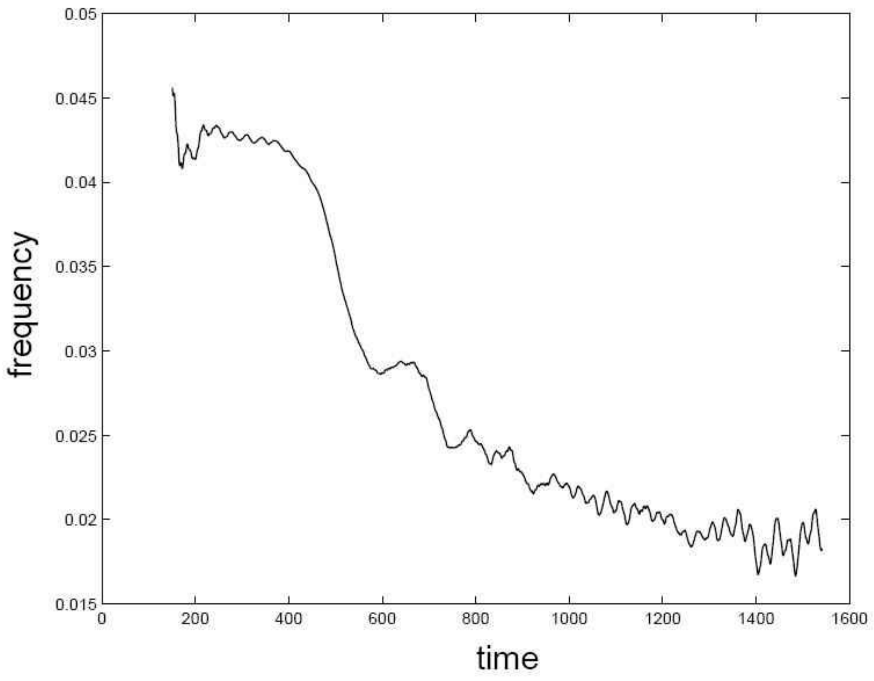

Simulation of fishbone driven by trapped beam ions in EAST plasmas

W. Shen, Nuclear Fusion 2017

Beam-driven fishbone in EAST experiment

- In 2014, the fishbone instability was observed in EAST experiment with NBI heating for the first time, and it was diagnosed by a solid-state neutral particle analyzer together with a soft X-ray system[1]. In this work, the global kinetic-MHD hybrid code M3D-K[2,3] is applied to study the fishbone instability in the EAST experiment.

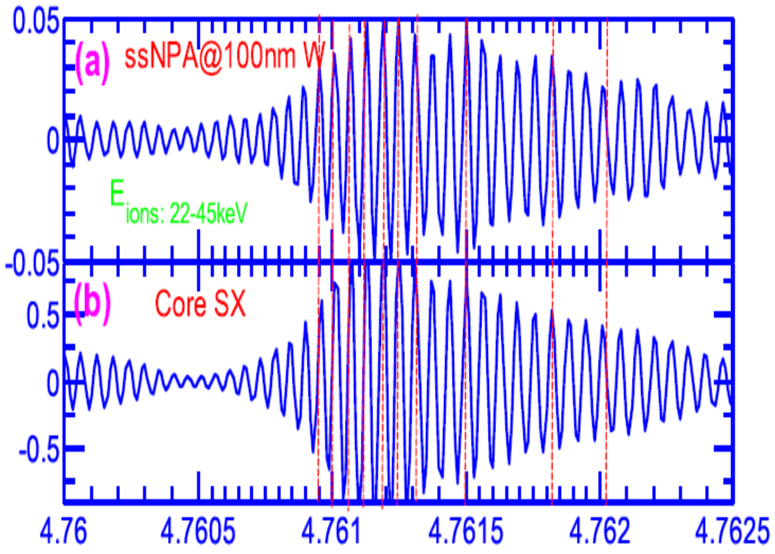

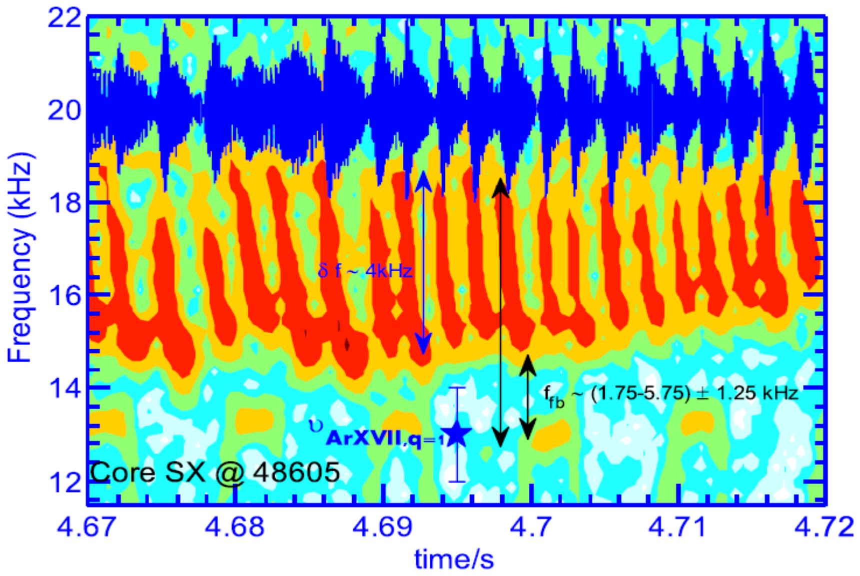

[1] Xu L.Q. et al 2016 Phys. Plasmas 22 122510
[2] Park W. et al 1999 Phys. Plasmas 6 1796
[3] Fu G.Y. et al 2006 Phys. Plasmas 13 052517

Basic parameters and initial profiles

Main parameters in EAST Shot #48605:

major radius: R_0=1.86 m

minor radius: a=0.44 m

elongation: κ=1.60

triangularity: δ=0.43

toroidal magnetic field: B_0=1.75 T

central density: $n_0=5.28\times10^{19}$ m^{-3}

central total plasma beta: $\beta_{total,0}$=3.45%

central beam ion beta: $\beta_{hot,0}$=0.86%

Beam ion distribution function:

$$f = c(\sum_{i=1}^{3} c_i \frac{H(v_0/\sqrt{i} - v)}{v^3 + v_c^3}) exp(-(\Lambda - \Lambda_0)^2/\Delta\Lambda^2) exp(-\langle\Psi\rangle/\Delta\Psi),$$

$$\Lambda \equiv \mu B_0/E \qquad \Lambda_0 = 0.8,\ \Delta\Lambda = 0.5,\ \Delta\Psi = 0.3,$$

- The injection energy of NBI is E_0 = 60 keV. Also NBI of $E_0/2$ and $E_0/3$ are included.

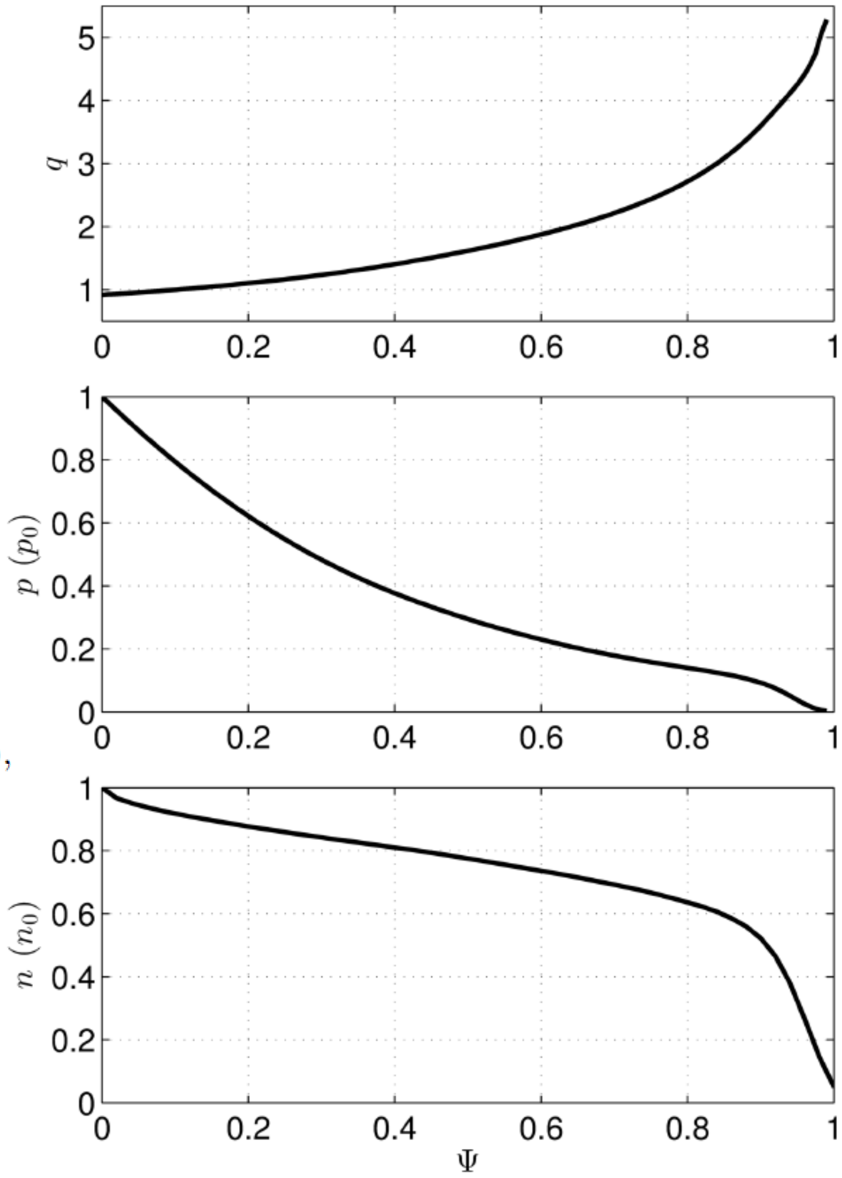

Linear results with different beam pressures

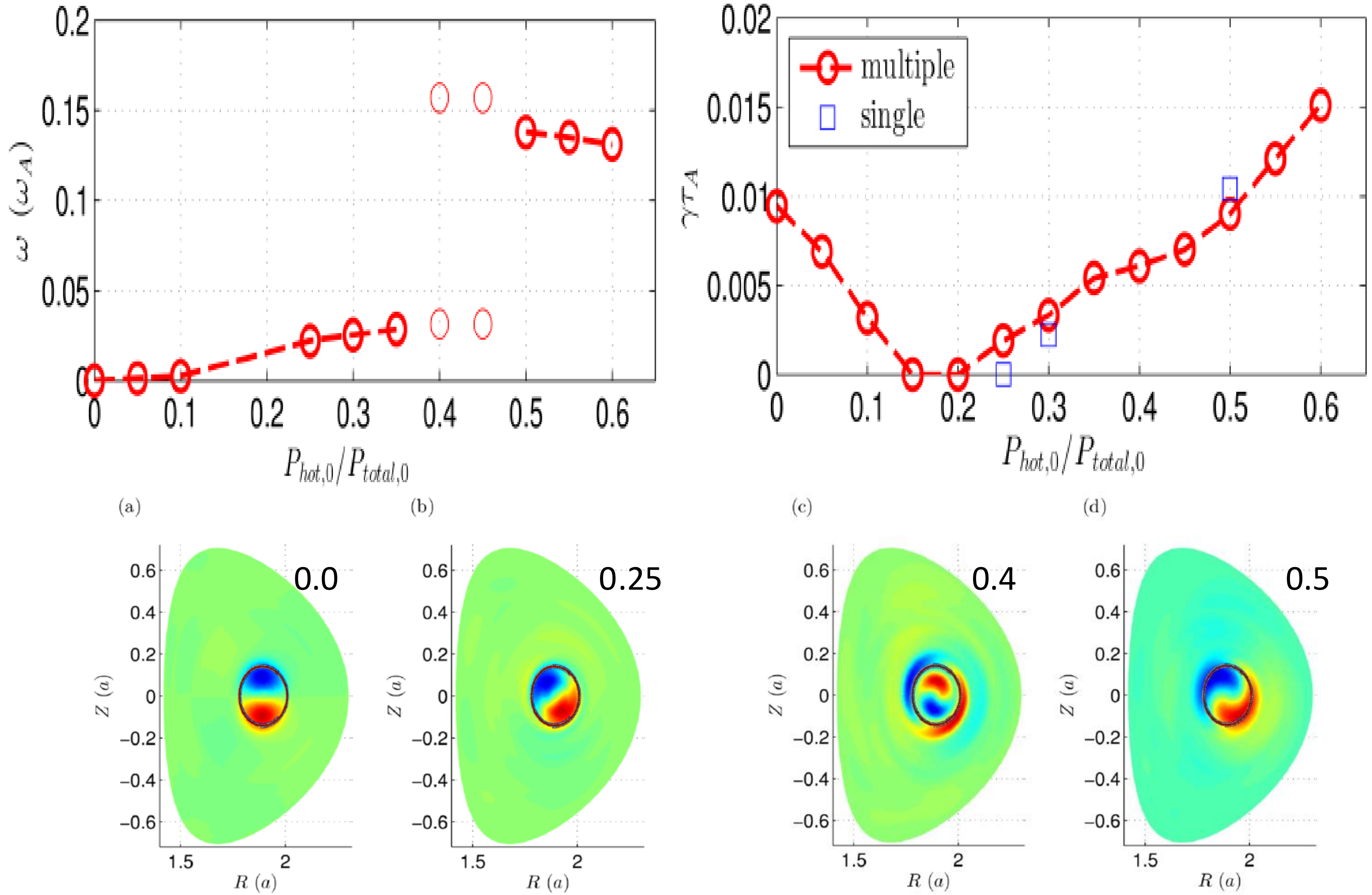

Simulation results agree well with experiment with respect to frequency and mode structure

- $P_{hot,0}/P_{total,0}$ is around 0.25 according to EAST experiment measurements. The corresponding simulated mode frequency is $f_{sim} = (0.022\ \omega_A)/(2\pi) = 6.99$ kHz. This is consistent with the experiment measured mode frequency of $f_{exp} = 5\sim7$ kHz

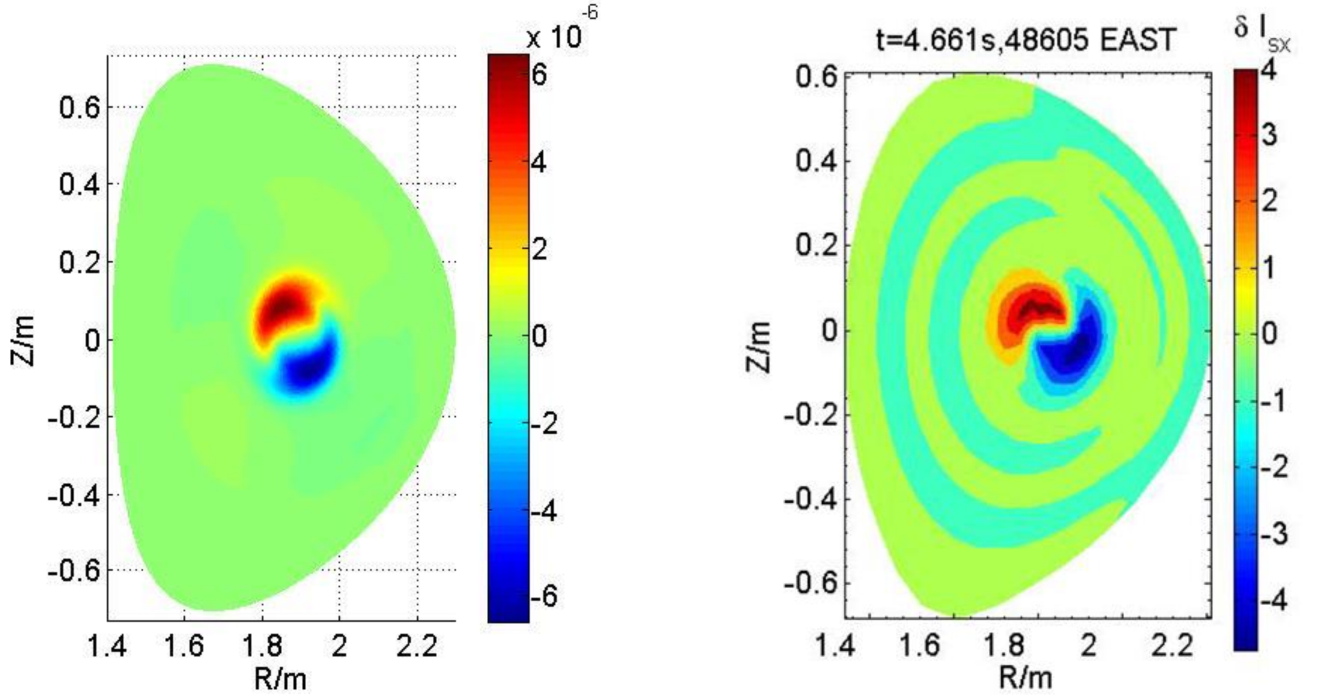

Nonlinear simulation shows frequency chirping and excitation of higher frequency mode

- The mode amplitude first grows and then saturates from t $\simeq$ 1500 τ_A.
- The mode frequency chirps up and down with the downward branch dominant.
- A new high frequency mode with $\omega \simeq 0.166\ \omega_A$ emerges at t $\simeq$ 3000 τ_A and persists around 2000 τ_A.
- The new high frequency mode was not observed in the EAST experiment, because the maximum mode frequency which can be measured in the experiment is around 0.117 ω_A

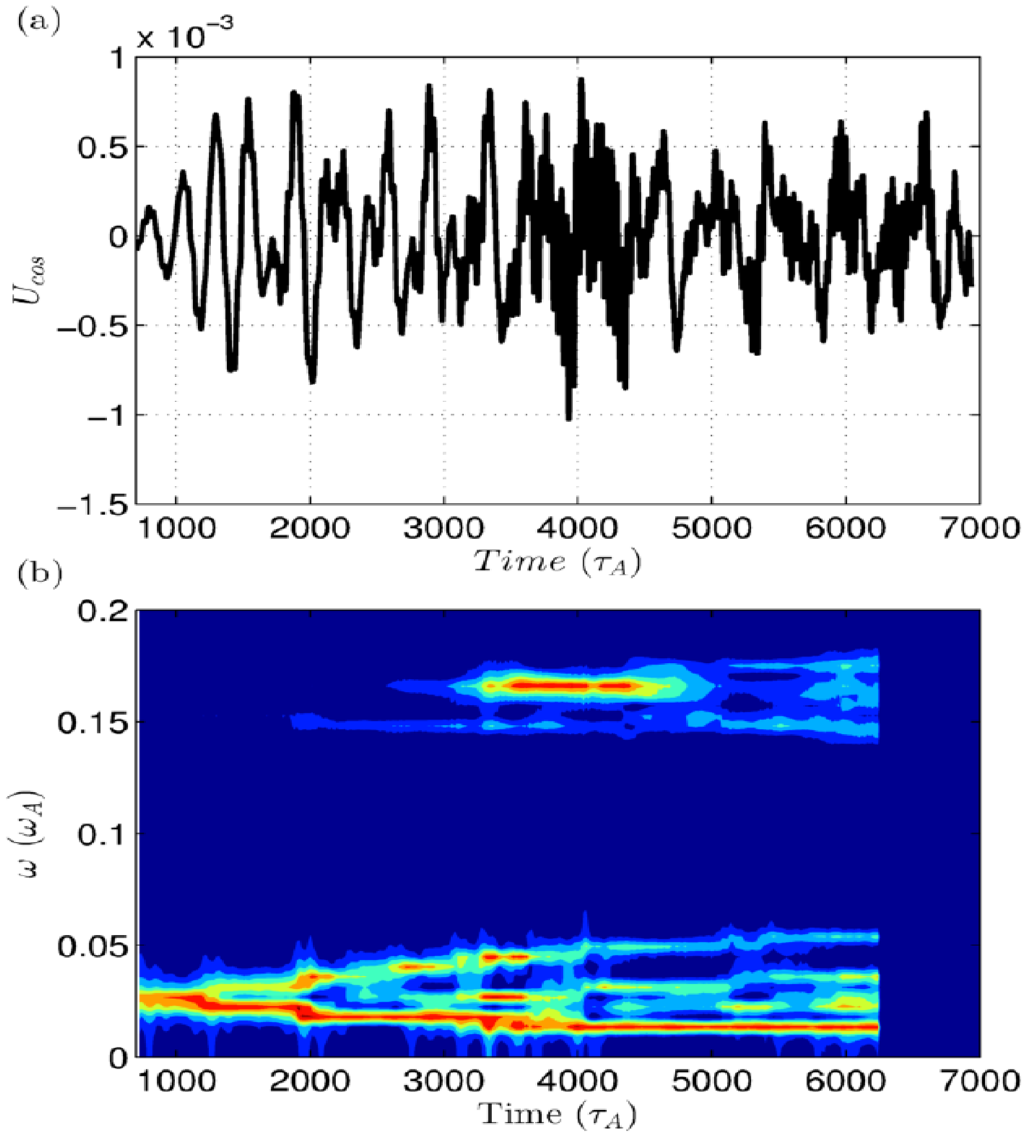

Nonlinear simulation shows frequency jumping

- In early nonlinear phase, the low frequency mode with $\omega \simeq 0.0314\ \omega_A$ is dominant until $t \simeq 1200\ \tau_A$.
- In later nonlinear phase $1200\ \tau_A \leq t \leq 2500\ \tau_A$, the high frequency $\omega \simeq 0.157\ \omega_A$ becomes dominant.
- Finally the mode transits to the low frequency mode with $\omega \simeq 0.0157\ \omega_A$ after $t \simeq 2500\ \tau_A$.

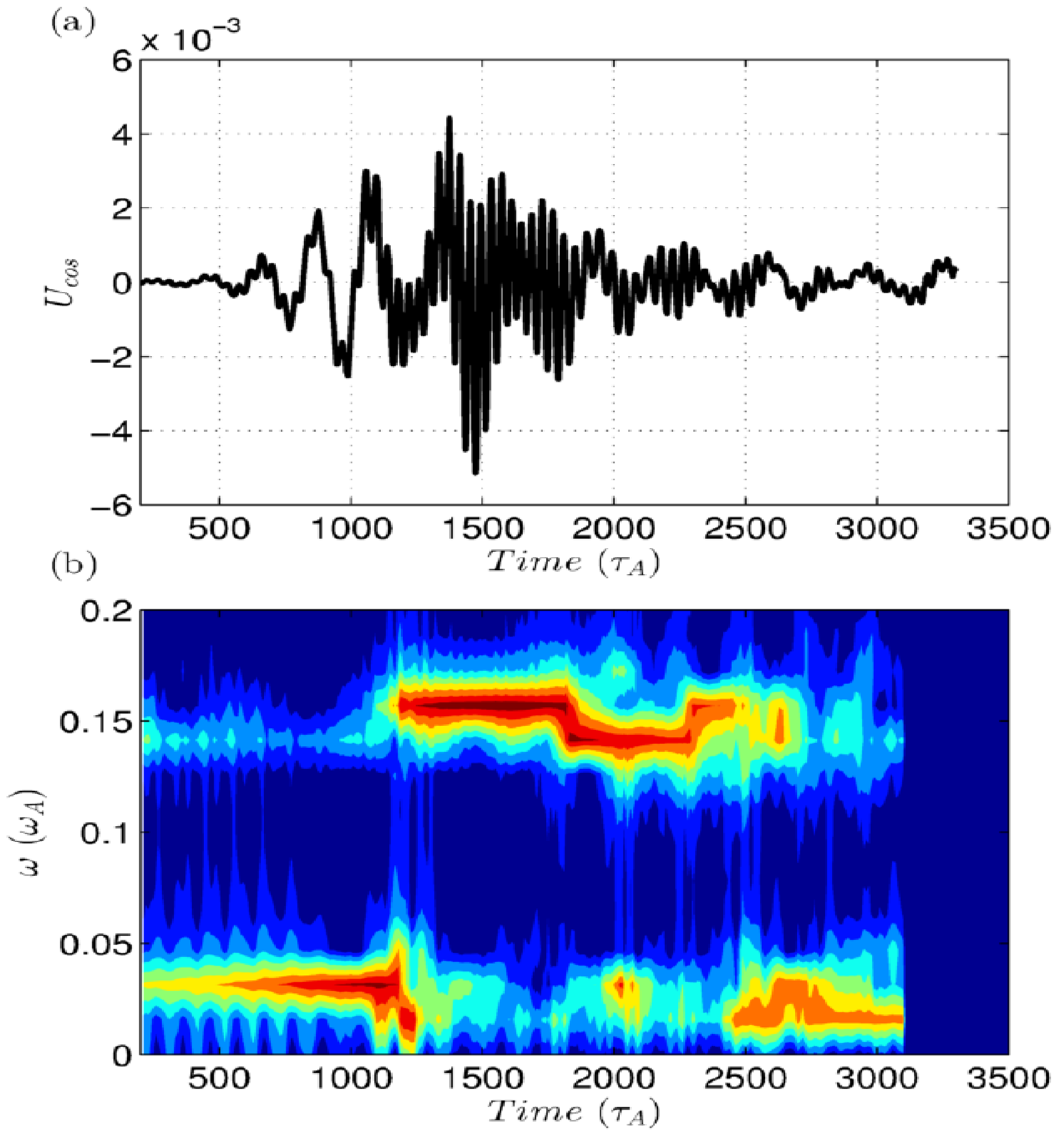

M3D-K simulations of sawteeth and energetic particle transport

W. Shen, G.Y. Fu, Z.M. Sheng, PoP 2014

- Sawteeth oscillations are periodic, internal magnetic reconnection events which occur in tokamak plasmas. They are mainly caused by internal kink mode with dominant toroidal and poloidal mode numbers n=m=1. Sawteeth can induce large energetic particle transport.

- Previous theoretical work

Kolesnichenko 1996: The E x B drift drives the redistribution whereas the precession weakens it when $\omega_d \tau_{crash} > 2\pi$ ($E > E_{crit}$);

Zhao and While 1997: ORBIT simulation based on model evolution of sawtooth crash. Important role of the stochasticity of magnetic field lines;

- This work: test particle model with sawtooth crash simulated self-consistently using full resistive MHD model

M3D-K Simulations of Sawteeth and Energetic Particle Transport: Trapped particle at $E=E_{crit}/4$

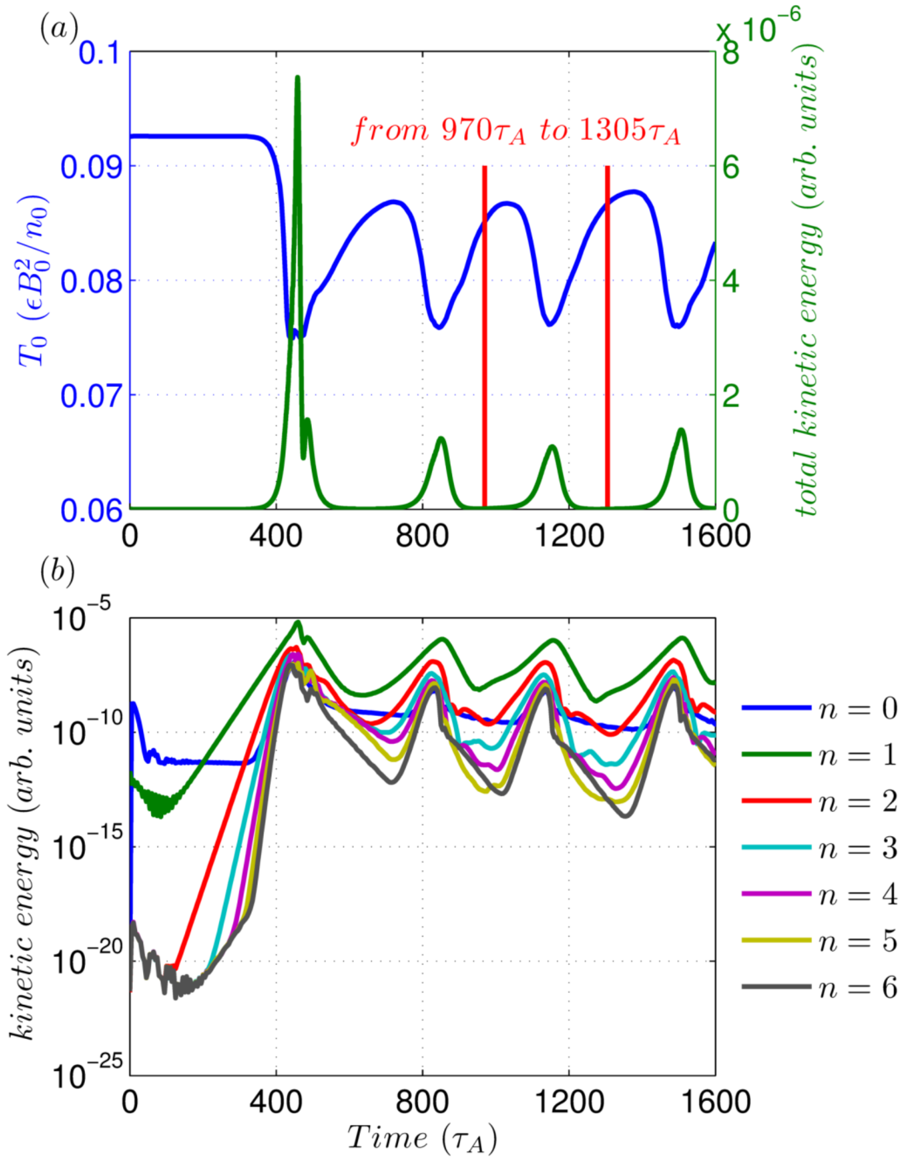

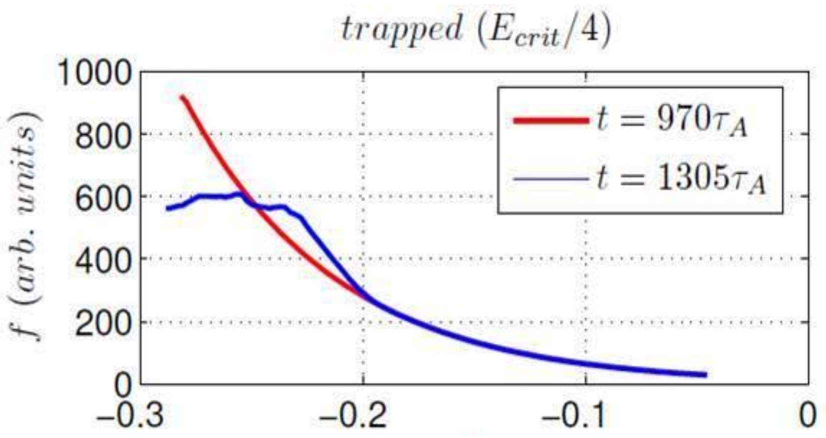

$P_\phi \sim \psi$

$E = E_{crit}$ at $\omega_d \tau_{crash} = 2\pi$

$\Lambda=\mu B_0 /E=1$

Sawtooth movie: Poincare plot and fast trapped ion distribution

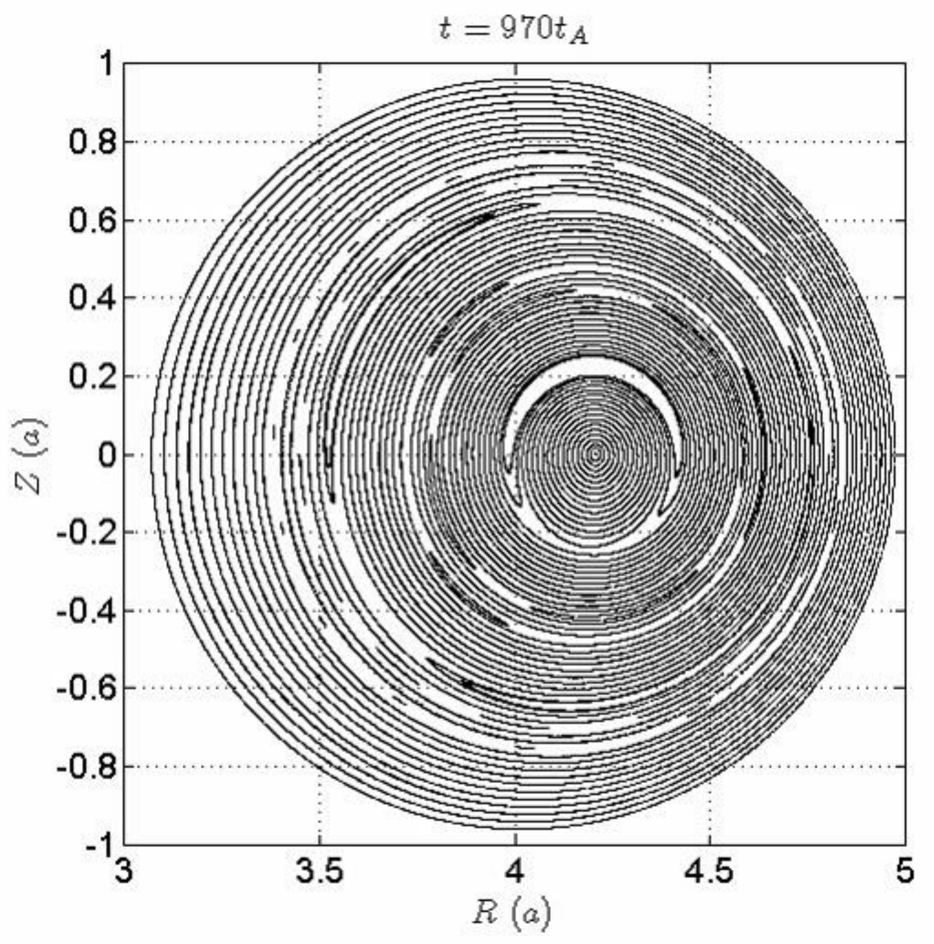

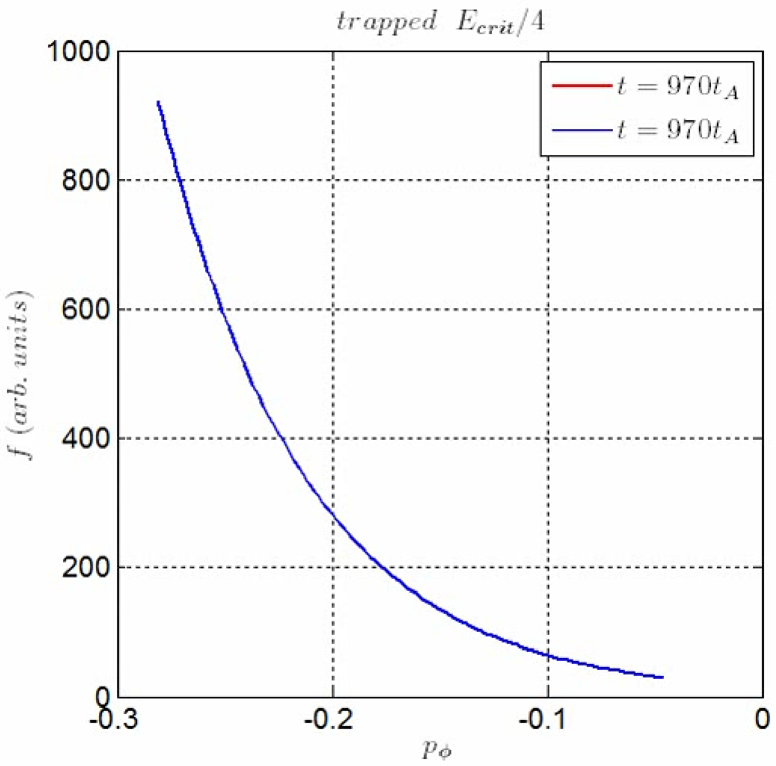

$P_\phi \sim \psi$

Energetic Particle Transport due to a sawtooth crash: strong energy dependence for trapped and counter-passing particles

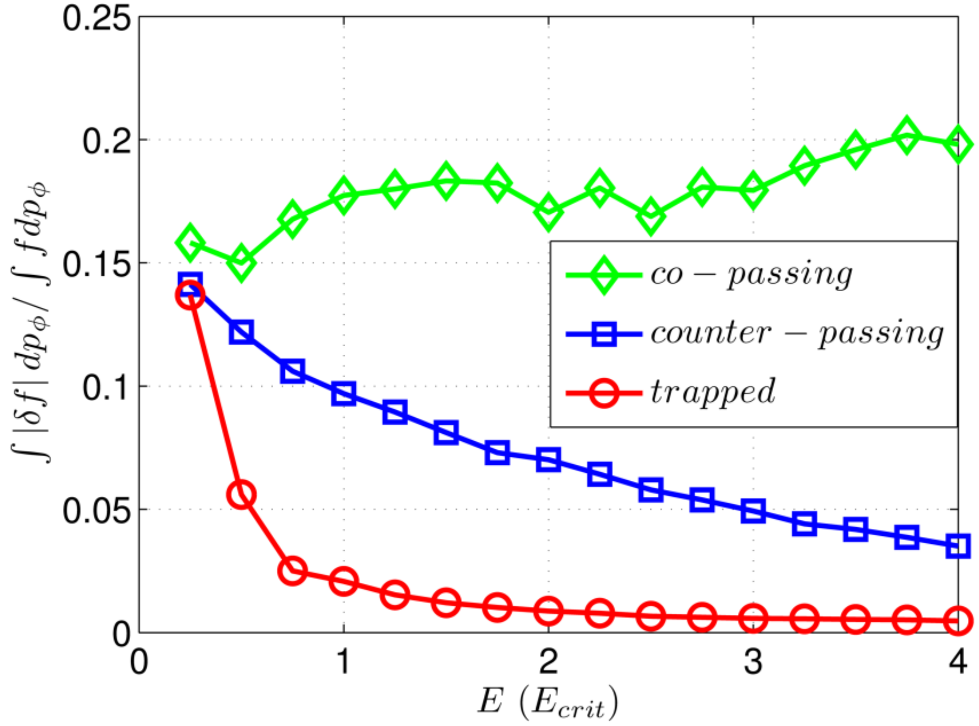

$$\int |\delta f| dP_\phi \,/ \int f dP_\phi = \frac{\int |f(t) - f(t = 970\tau_A)| dP_\phi}{\int f(t = 970\tau_A) dP_\phi}$$

$E = E_{crit}$ at $\omega_d \tau_{crash} = 2\pi$

$\Lambda = \mu B_0 / E$ passing particles with $\Lambda=0$; trapped particles with $\Lambda=1.0$

Summary :M3D-K Simulations of Sawteeth and Energetic Particle Transport

- MHD simulations show repeated sawtooth cycles due to a resistive (1,1) internal kink mode for a model tokamak equilibrium.
- Test particle simulations are carried out to study the energetic particle transport due to a sawtooth crash.
- For trapped particles, the redistribution occurs for particle energy below a critical value in agreement with previous theory.
- For co-passing particles, the redistribution is strong with little dependence on particle energy. In contrast, the redistribution level of counter-passing particles decreases as particle energy becomes large.

Energetic particle transport due to kink mode and Fishbone in NSTX (F. Wang et al, PoP 2013)

- We consider NSTX plasmas with a weakly reversed q profile and q_min close but above unity.
- For such q profile, fishbone and non-resonant kink mode (NRK) have been observed in NSTX and MAST.
- Experiment results showed that kink mode and fishbone can drive large beam ion redistribution (NSTX and MAST)

Equilibrium profile and parameters :

NSTX #124379 at t=0.635s

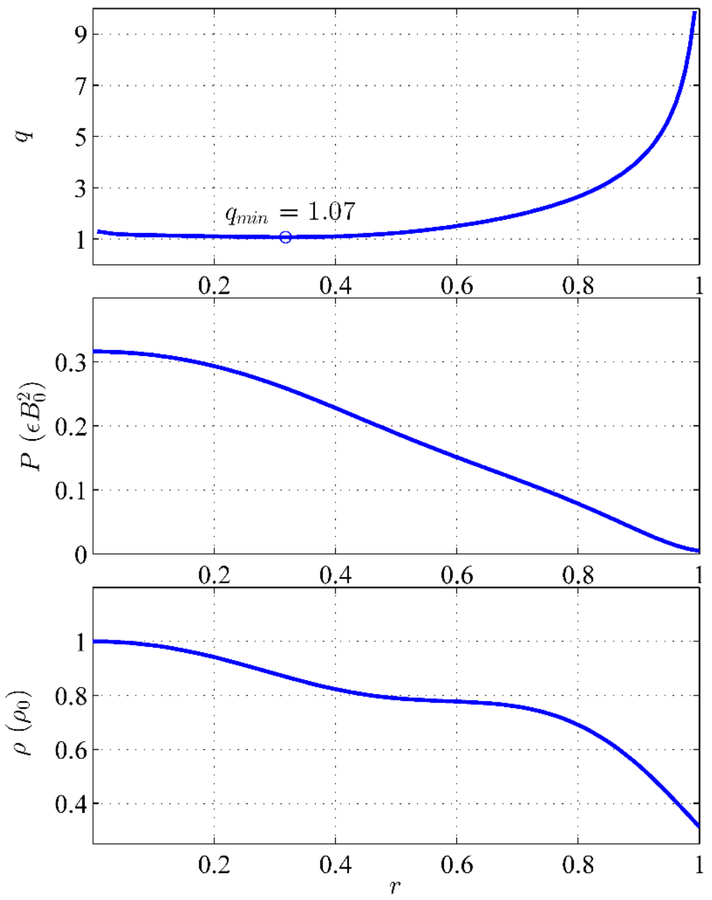

$$\beta \sim 0.3$$
$$q_{\min} \sim 1.03 \rightarrow 1.2$$
$$R_0 = 0.858m$$
$$a = 0.602m$$
$$B_0 = 0.44T$$
$$n_0 = 9.3 \times 10^{19} m^{-3}$$

$$\eta(T) = \eta_0 (T/T_0)^{-3/2}$$
$$\eta_0 = 5 \times 10^{-6}$$
$$\mu = 1 \times 10^{-4}$$
$$\chi_\perp = 5 \times 10^{-5}$$

Beam-driven fishbones and non-resonant kink modes (LLM) are observed in NSTX and MAST

E. Fredrickson

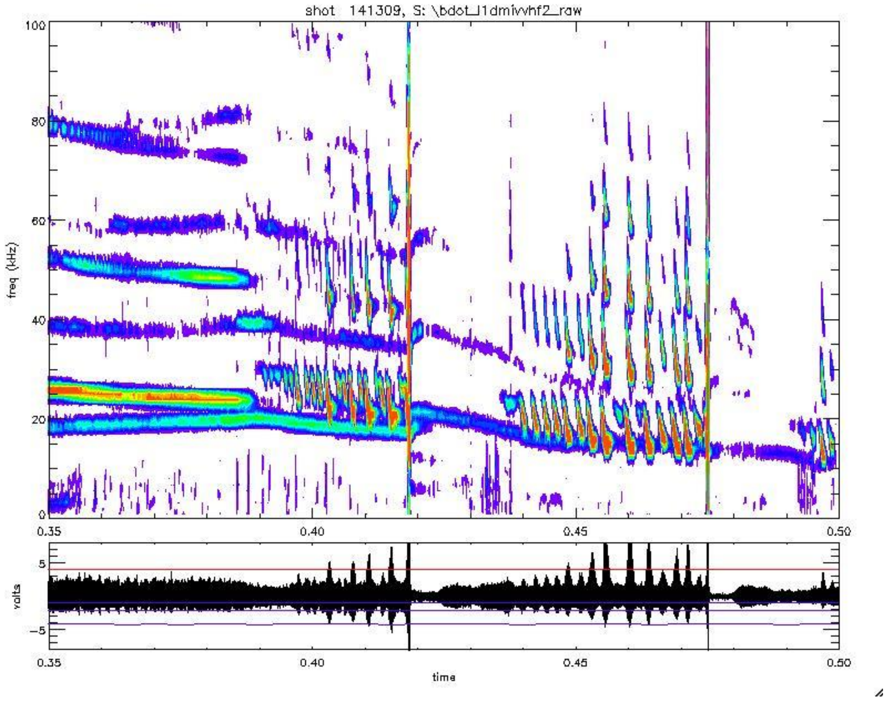

I.T. Chapman et al., Nucl. Fusion, 2010

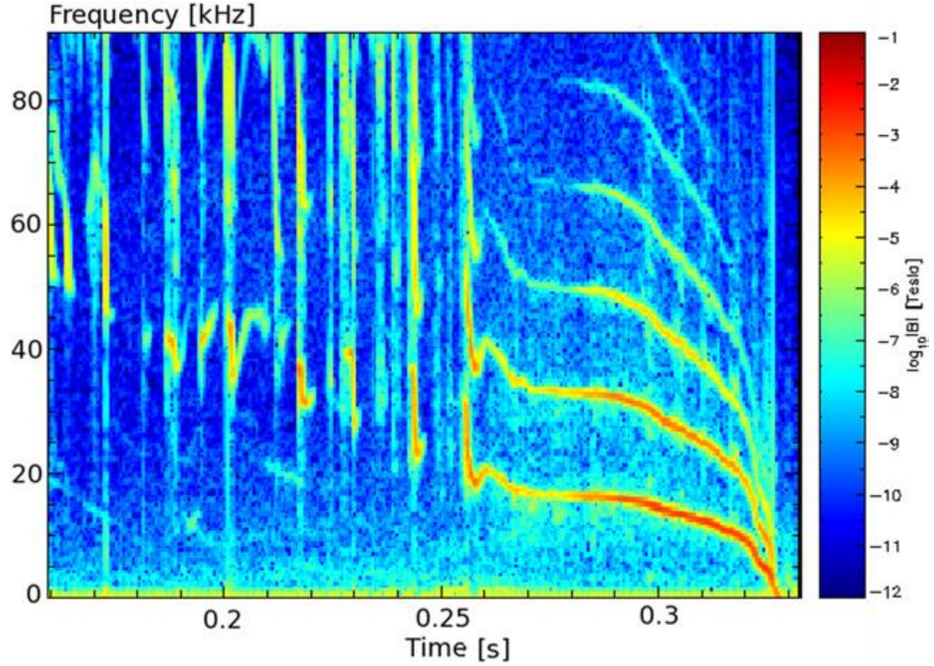

The fishbone mode structure shows twisting feature

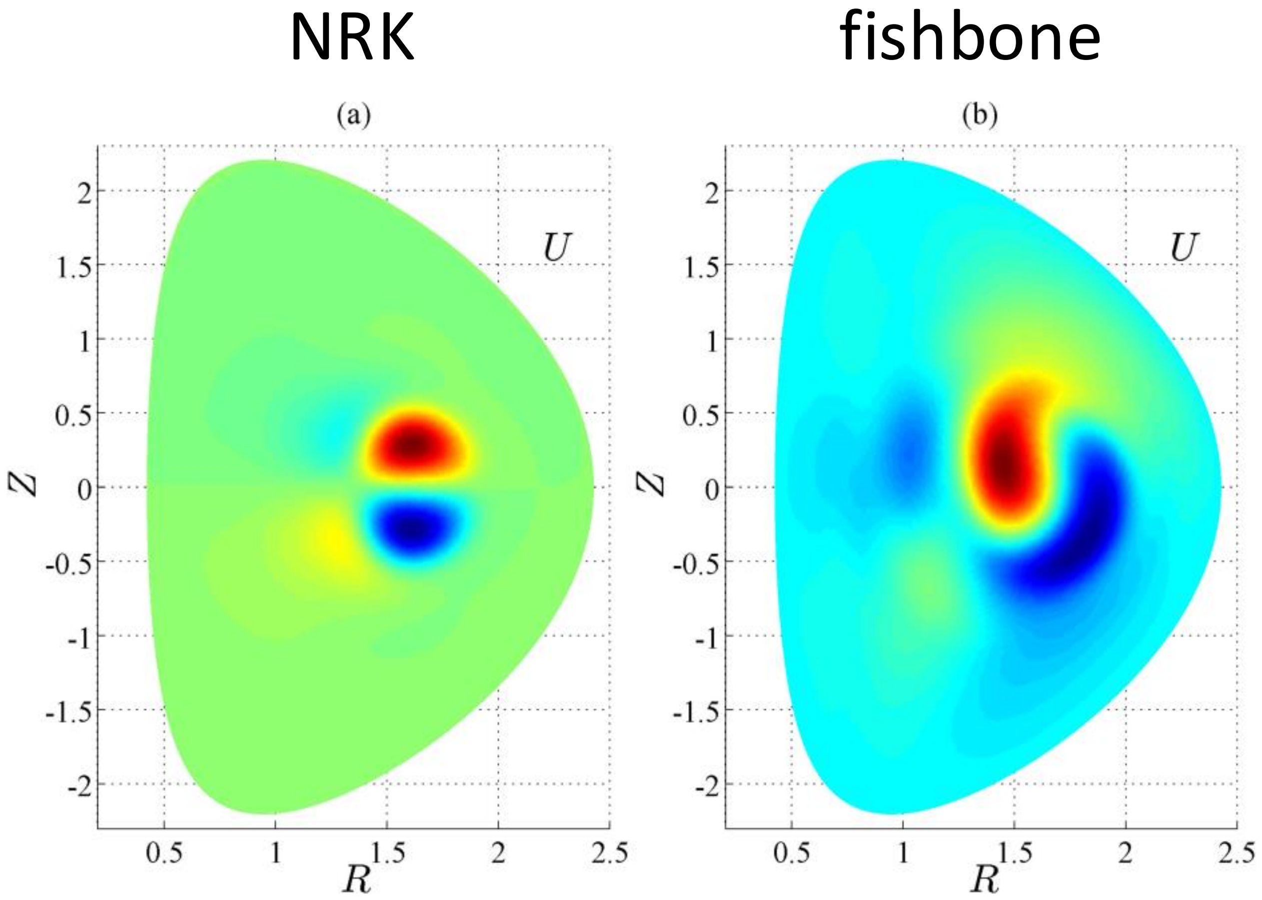

Stability diagram: stabilization of ideal kink and excitation of fishbone at higher q_min

At fixed P_total at axis

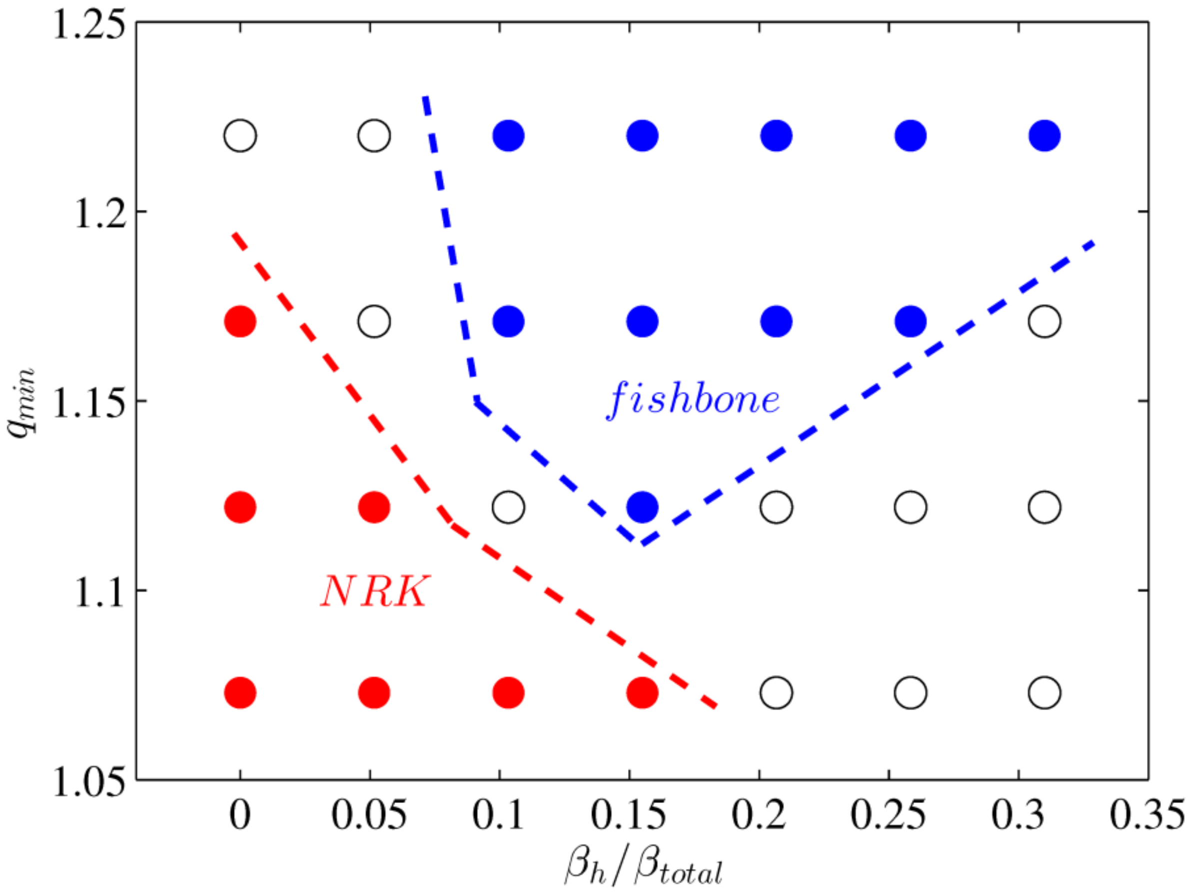

Steady state saturation of NRK with beam ions

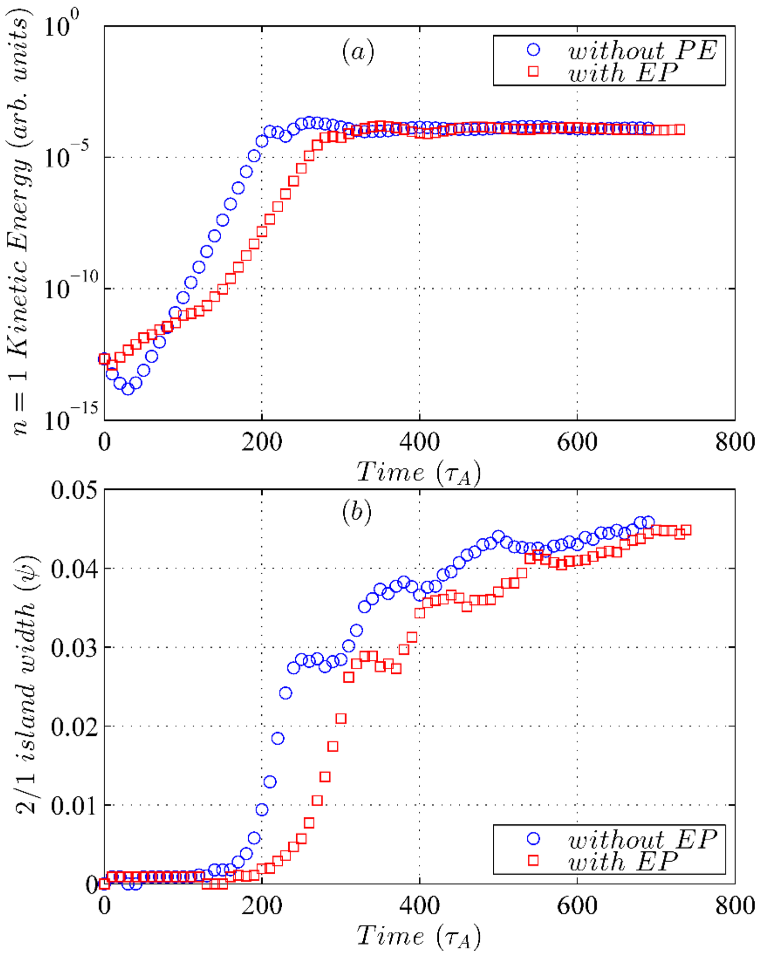

Energetic particles have weak effects on the NRK mode nonlinear saturation level (including the n=1 kinetic energy and the 2/1 island width) .

NRK drives significant redistribution of passing particles

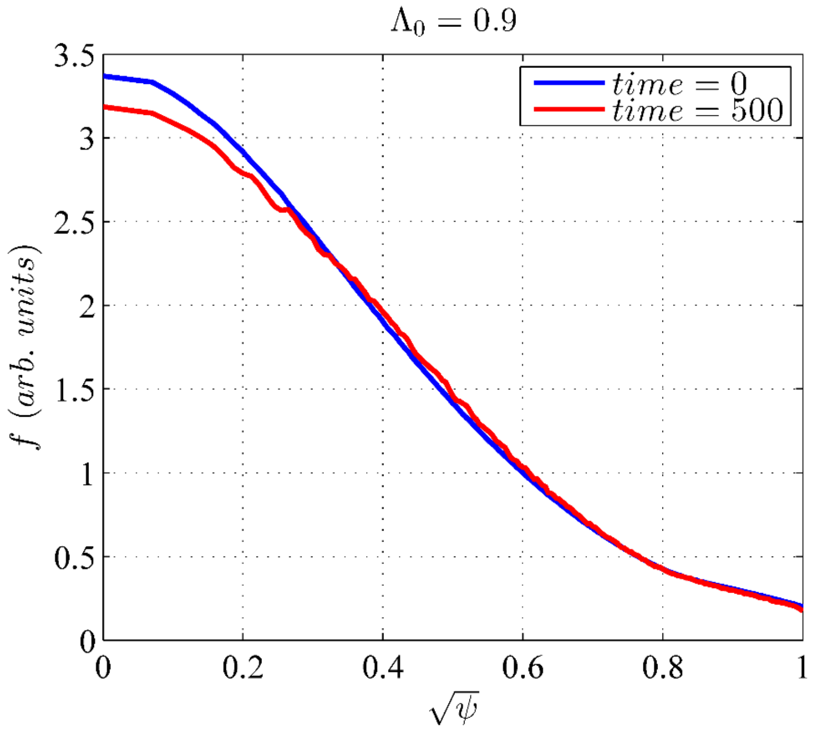

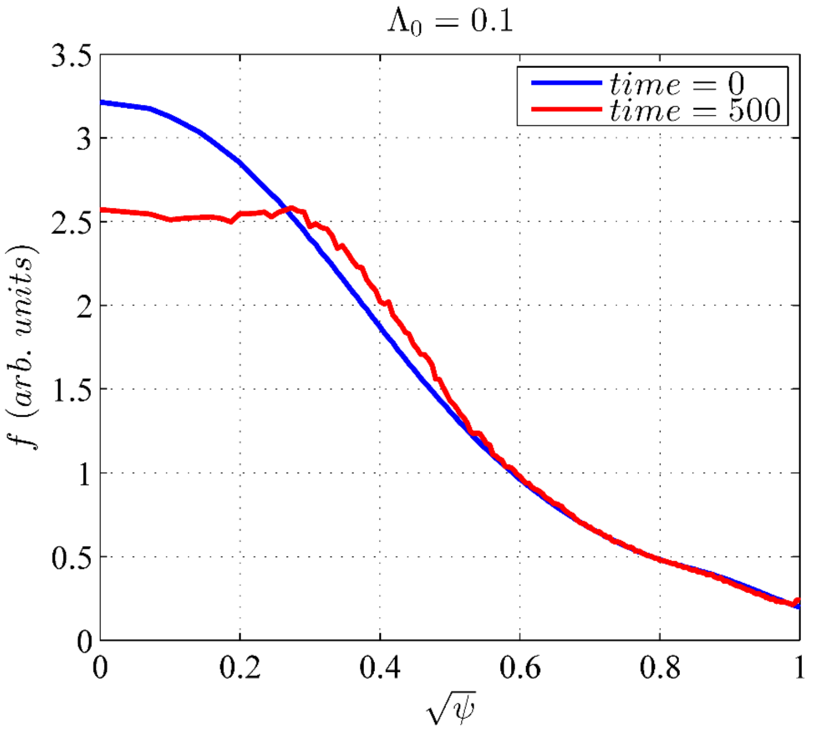

Fishbone nonlinear evolution

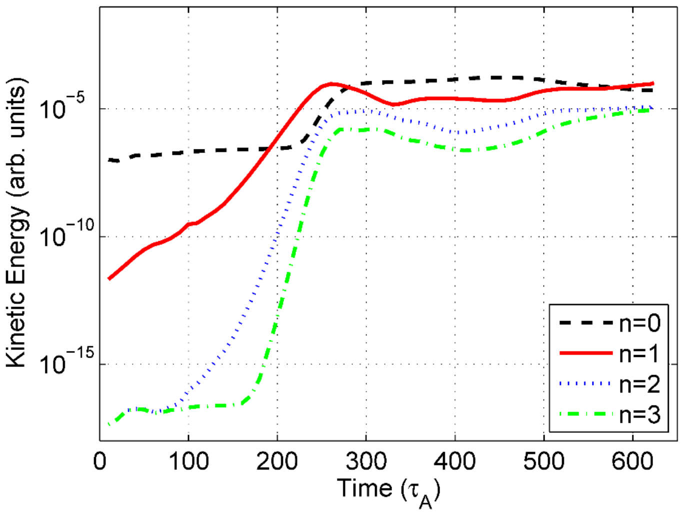

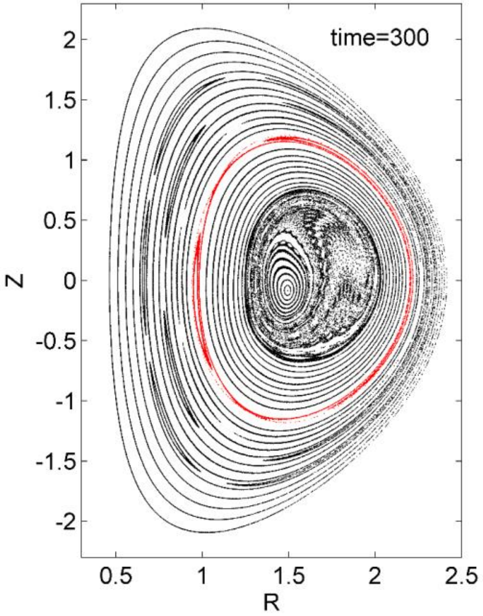

Nonlinearly, the fishbone shows strong frequency chirping, and induces 2/1 island, which could trigger NTM.

It induces strong beam ion profile flattening in the core.

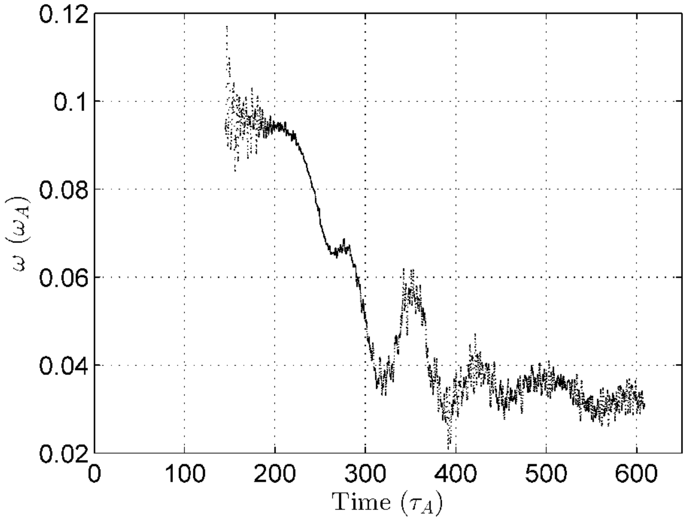

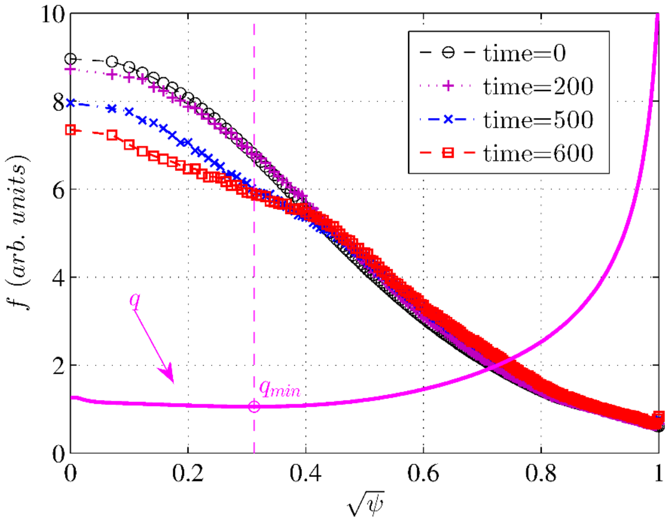

Theory of low-frequency fishbone driven by passing beam ions in HL-2A plasmas

- Recent HL-2A Results show a low frequency fishbone is excited by passing beam ions;
- Motivated by HL-2A results, a fishbone dispersion relation is derived, solved, and applied to the HL-2A experiment.

L.M. Yu, Nuclear Fusion 2019

Recent HL-2A Results show a low frequency fishbone is excited by beam ions

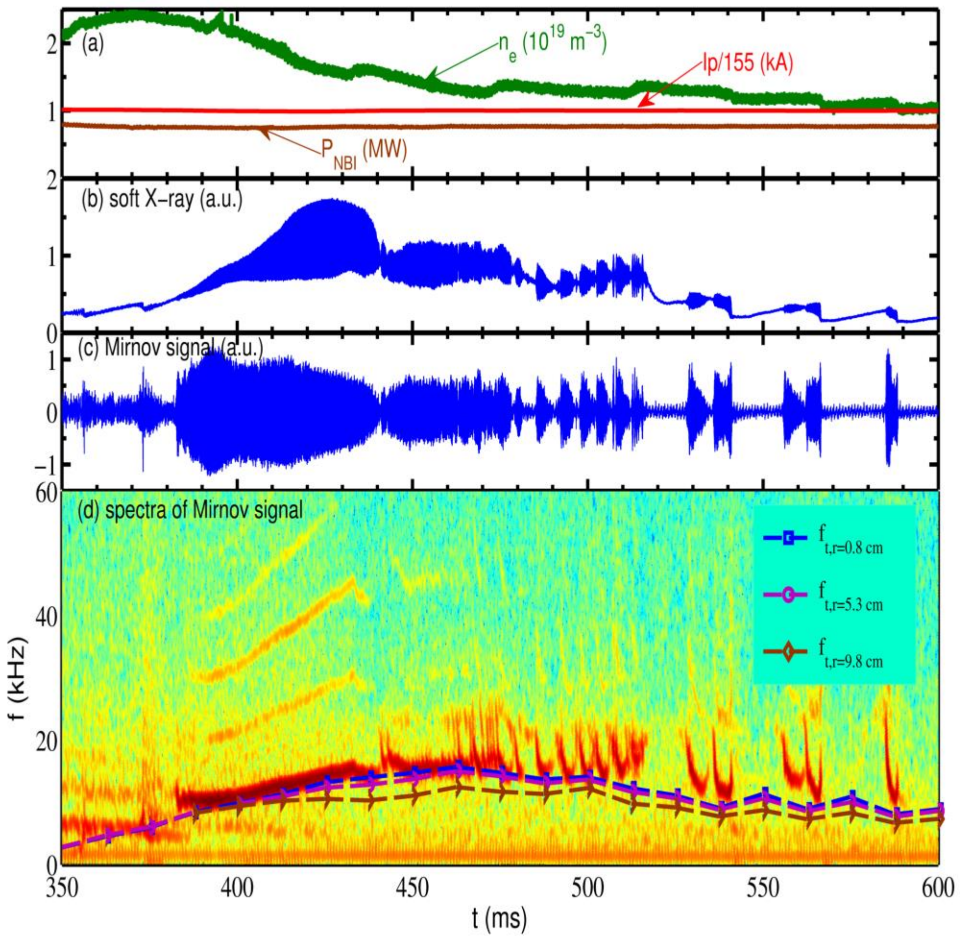

HL-2A,22485

Discharge 22485, t=600~650 f(fishbone)=25kHZ
in plasma frame, the initial frequency o fishbone: f(fishbone)~10kHZ

Fishbone dispersion relation

$$-i\frac{\omega}{\tilde{\omega}_A} + \delta\hat{W}_f + \delta\hat{W}_k = 0$$

$$\delta W_k = \frac{1}{2}\int d^3x\vec{\xi}^* \cdot \nabla\,\delta P_k$$

$$\delta P_{k\perp} = \int d^3v\frac{1}{2}Mv_\perp^2 g$$

$$\delta P_{k\|} = \int d^3v M v_\|^2 g$$

g : the non-adiabatic distribution function of hot ions

Drift kinetic equation of g with FOW for m=1,n=1 fishbone

$$\left(\partial_t + v_d \cdot \nabla + v_\parallel b \cdot \nabla\right) g = i\varepsilon \frac{\partial F}{\partial \varepsilon}\left(\omega - \omega_*\right) G$$

$$G(r,\theta,\Lambda) = \left[\Lambda / b + 2\left(1 - \Lambda / b\right)\right] \kappa \cdot \xi$$

$$\xi = \left[\xi_r(r,\theta)\nabla r + \xi_\theta(r,\theta)\nabla\theta\right]\exp\left[i\left(\phi - \omega t\right)\right]$$

$$\xi_r(r,\theta) = \xi_0 H\left(r_s - \langle r \rangle - \rho_d \cos\theta\right)\exp\left(-i\theta\right)$$

$$\xi_\theta(r,\theta) = -ir\xi_0 H\left(r_s - \langle r \rangle - \rho_d \cos\theta\right)\exp\left(-i\theta\right)$$

FOW

The formula of δW_k

$$\delta W_k = \int \frac{J}{q} dx\, d\Lambda\, \varepsilon^3 d\varepsilon \frac{\partial F}{\partial \varepsilon} \tau_b \left(\omega - \omega_*\right) \sum_{p,\sigma} \frac{\left|Y_p^\sigma\right|^2}{n\omega_\phi + p\omega_\theta - \omega}$$

$$F = \frac{p_h(x)}{\pi n_0 T_h \varepsilon_0} \frac{1}{\varepsilon^{3/2}} H\left(\varepsilon_0 - \varepsilon\right) \delta\left(\Lambda\right)$$

- The slowing-down distribution function for beam ions is considered.
- For low-frequency fishbone, the p=0 and p=-1 terms of δW_k are included.

Fishbone dispersion relation is derived

$$-i\frac{\hat{\Omega}}{\tilde{\Omega}_A} + \delta\hat{W} = 0 \qquad \hat{\Omega} = \frac{\bar{\omega}}{\frac{s}{q_s r_s}\Delta_b}, \; \bar{\omega} = \omega R/v_h$$

$$\tilde{\Omega}_A = \tilde{\omega}_A/\left(\frac{v_h}{R}\frac{s}{q_s r_s}\Delta_b\right) \qquad \tilde{\omega}_A = v_A/3^{1/2}R_0\hat{s}$$

$$\delta\hat{W} = \delta\hat{W}_T + \frac{1}{2}\pi\varepsilon_1^2\beta_{ph} + \frac{1}{3}\pi\varepsilon_1\left(\frac{\Delta_b}{r_p}\right)_s\tilde{\beta}_{phs}\left[A - \frac{2F\left(\hat{\Omega}\right)}{\pi s_1}\right]$$

toroidal — anisotropic — finite orbit width — asymmetric — resonance

Graves PRL 2004

$$\delta\hat{W}_T = 3\pi\left(1 - q_0\right)\left(\frac{r_s}{R_0}\right)^2\left(\frac{13}{144} - \beta_{ps}^2\right)$$

$$\beta_{ps} = -\frac{2\mu_0}{B_0^2\varepsilon_1^2}\int_0^{r_s} dr\left(\frac{r}{r_s}\right)^2\frac{d\left\langle P\right\rangle}{dr}$$

$$\left\langle P\right\rangle = \left\langle P_h\right\rangle + P_c$$

$$P_h \equiv \frac{P_{h\parallel} + P_{h\perp}}{2}$$

$$\left\langle P\right\rangle \equiv \frac{1}{2\pi}\int_0^{2\pi} d\theta P$$

$$\beta_{ph} = -\frac{2\mu_0}{B_0^2\varepsilon_1^2}\int_0^{r_s} dr\left(\frac{r}{r_s}\right)^2\frac{d\left\langle P_h\right\rangle}{dr}$$

$$\tilde{\beta}_{phs} = \frac{2\mu_0\left\langle P_h\right\rangle(r_s)}{B_0^2\varepsilon_1^2}$$

Effects of Finite Orbit Width

- Responsible for P=-1 resonance
- Stabilizing for co-passing ions due to good curvature

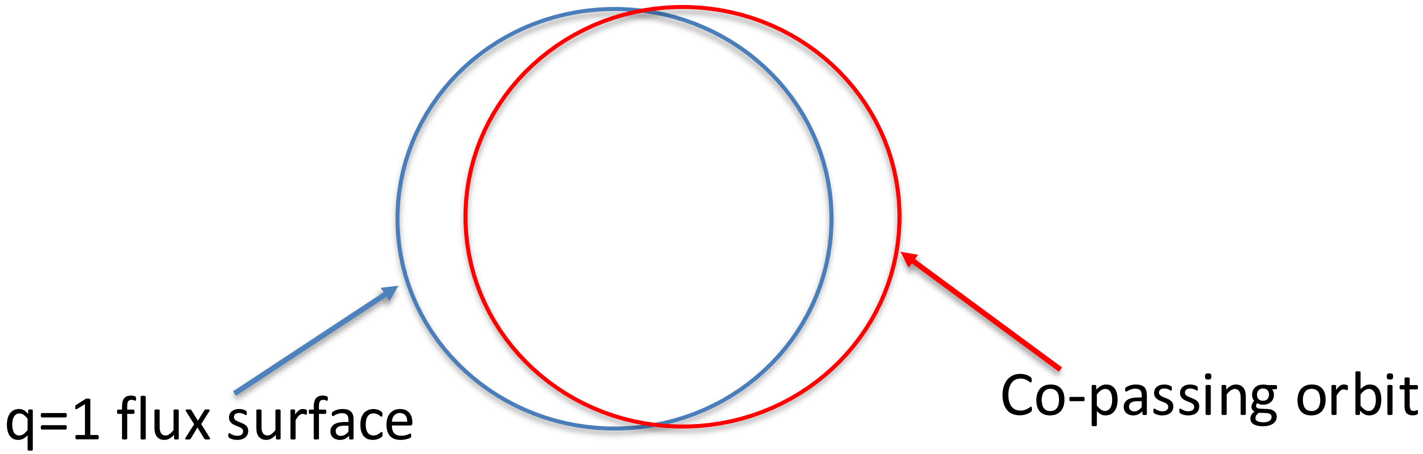

$$F\left(\hat{\Omega}\right) = \frac{1}{\pi}\left\{-8\hat{\Omega}^{\frac{3}{2}}\left[\tan^{-1}\frac{1}{\sqrt{\hat{\Omega}}} + \tanh^{-1}\frac{1}{\sqrt{\hat{\Omega}}}\right]\right.$$
$$\left. + \left(1+3\hat{\Omega}^2\right)\ln\left(\frac{\hat{\Omega}+1}{\hat{\Omega}-1}\right) + 10\hat{\Omega}\right\},$$

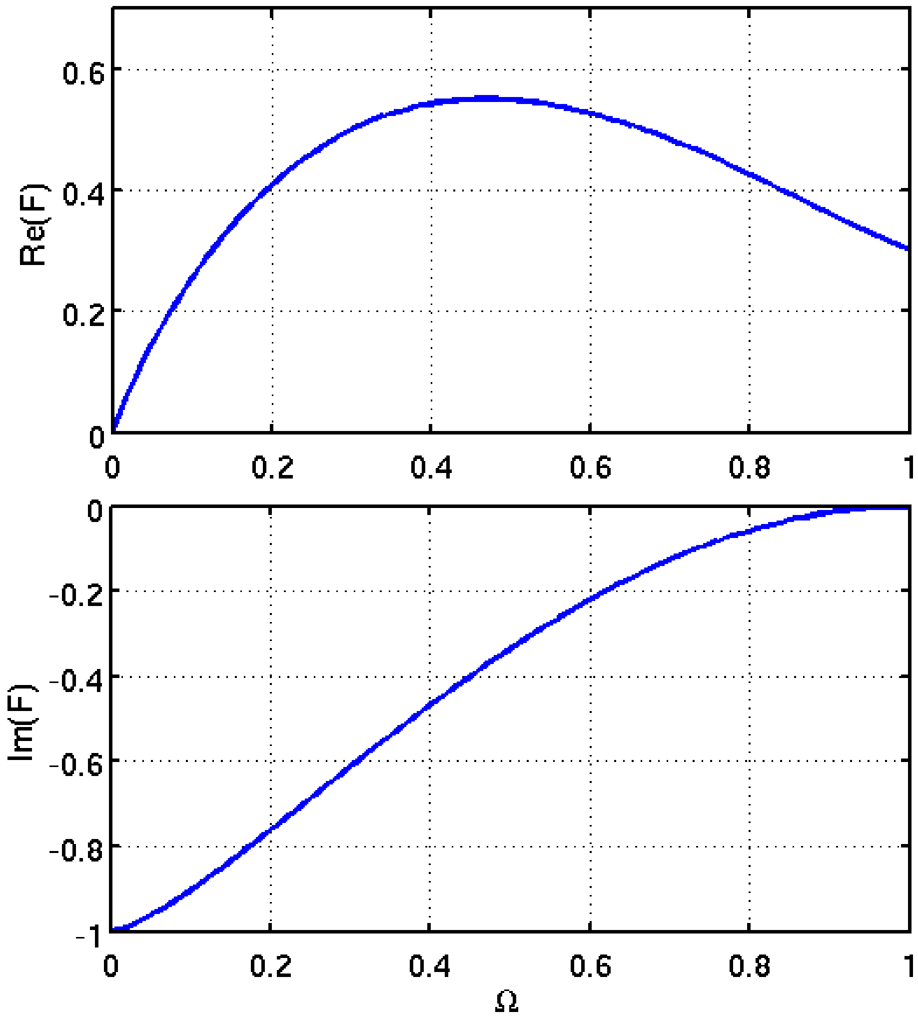

Betti PPCF 1993

For $\hat{\Omega} = \hat{\Omega}_r + i\hat{\Omega}_i$ and $\hat{\Omega}_i \ll \hat{\Omega}_r$, yields

$$-\frac{\hat{\Omega}_r}{\tilde{\Omega}_A} + \frac{1}{3}\pi\varepsilon_1 \frac{\Delta_b}{r_p}\tilde{\beta}_{phs}\left[-\frac{2\mathbf{Im}F\left(\hat{\Omega}\right)}{\pi s_1}\right] = 0$$

$$\frac{\hat{\Omega}_i}{\tilde{\Omega}_A} + \delta\hat{W}_T + \frac{1}{2}\pi\varepsilon_1^2\beta_{ph} + \frac{1}{3}\pi\varepsilon_1 \frac{\Delta_b}{r_p}\tilde{\beta}_{phs}\left[A - \frac{2\mathbf{Re}F\left(\hat{\Omega}\right)}{\pi s_1}\right] = 0$$

HL-2A Discharge 22485, t=600~650 parameters

- Bt =1.34T
- Ne=1.31e13 /cm^3 (Deuterium plasma)
- Ti=1750Ev
- Te=810Ev
- Beta=0.78%
- R0=1.65
- V_a=5.7070e6 m/s
- V_0=1.425e6 m/s
- f_0=142KHz
- T(se) slowing down time ~50ms
- Global energy confinement time ~50ms

- NBI injection 41~40KeV
- Pitch angle ~0.28
- Passing >90%
- $q=q0+2(r/a)^2$

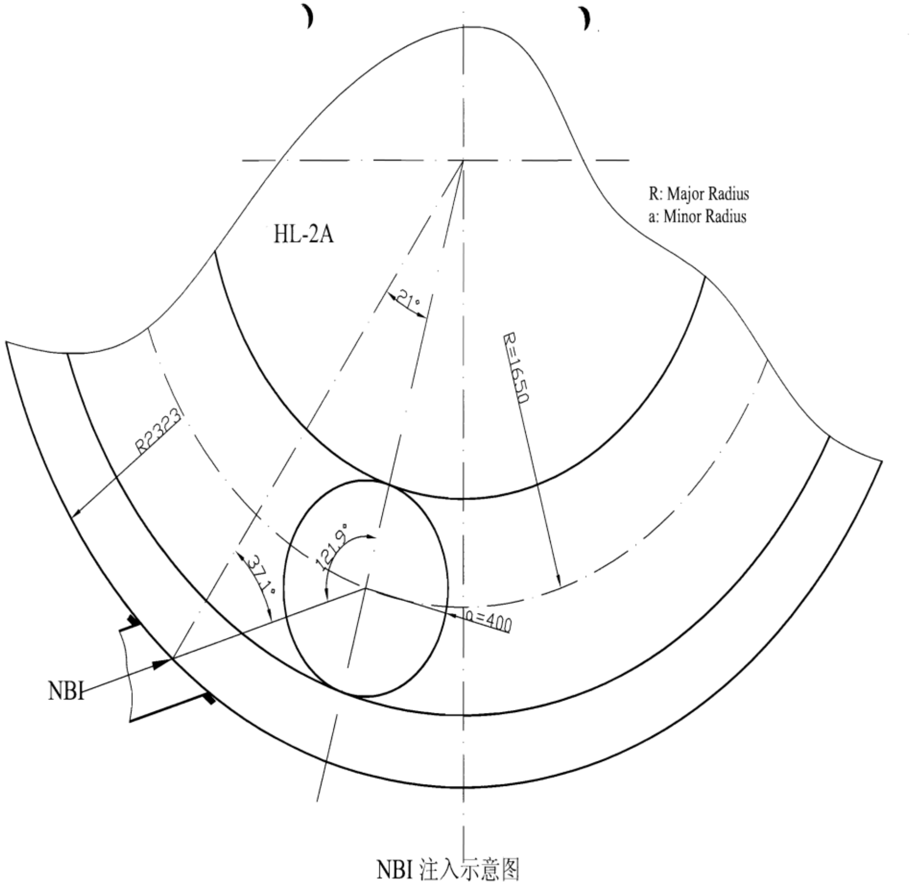

Solutions of dispersion near critical shear

s=0.28 s=0.30 s=0.32

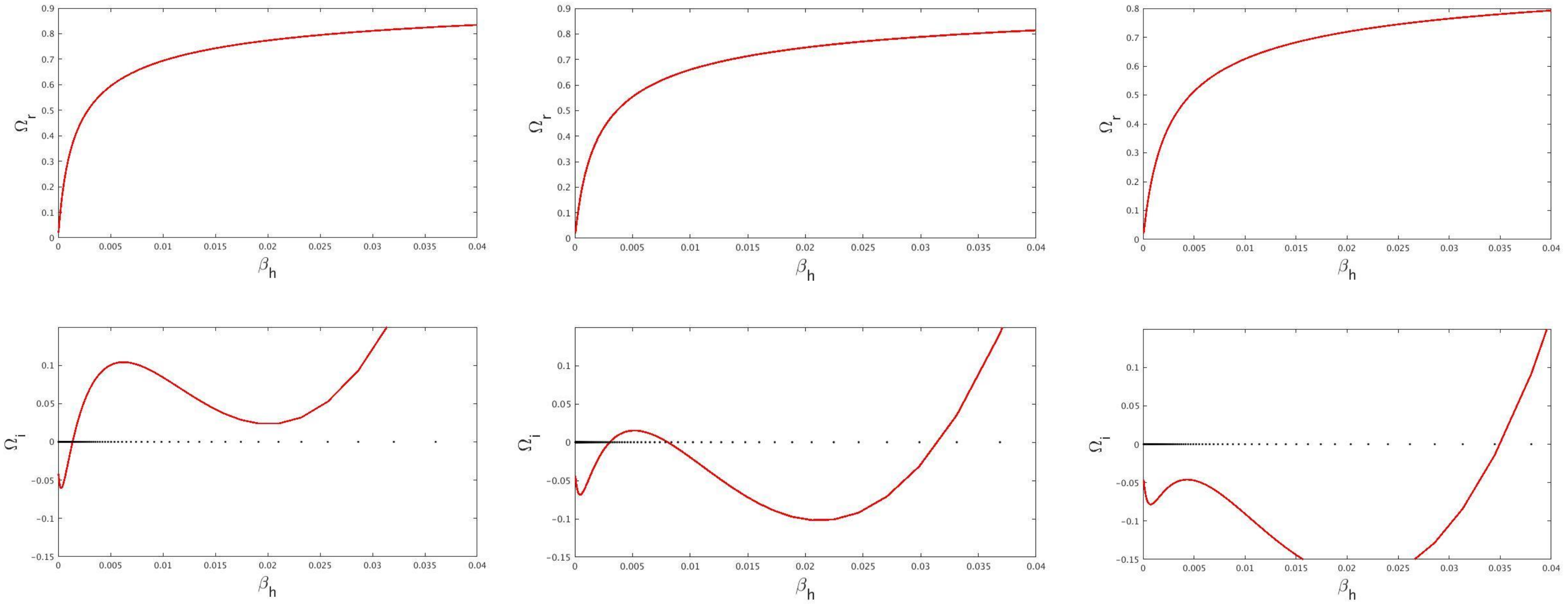

Critical shear for existence of the lower frequency branch with corresponding lower fast ion beta threshold

$$\frac{\hat{\Omega}_i}{\tilde{\Omega}_A} + \delta\hat{W}_T + \frac{1}{2}\pi\varepsilon_1^2\beta_{ph} + \frac{1}{3}\pi\varepsilon_1\frac{\Delta_b}{r_p}\tilde{\beta}_{phs}\left[A - \frac{2\mathbf{Re}F\left(\hat{\Omega}\right)}{\pi s_1}\right] = 0$$

The condition for critical shear is approximately determined by the sign of the last term.

$$S_{crit} = 2(\mathrm{Re}(F))_{max} / \pi A$$

Results for beam-driven fishbone in HL-2A

- $q = q0 + 2(r/a)^2$
- There exists a critical threshold in magnetic shear, s_{cirt} ~ 0.3 below which beta threshold of fast beam ion for fishbone excitation is very low, $\beta_{h,crit} < 0.5\%$;
- Above the critical shear, the beta threshold is much higher, on order of 3.0%;
- Mode frequency is similar to observed value ~ 10kHz.

Summary

- Motivated by HL-2A results of beam-driven fishbone, a fishbone dispersion relation of passing fast ion-driven fishbone is derived.
- There exists a critical threshold in magnetic shear for co-injection below which beta threshold of fast beam ion for fishbone excitation is quite low, $\beta_{h,crit} < 1\%$;
- Above the critical shear, the beta threshold is much higher.
- The estimated mode frequency is consistent with the observed value.
- According to our estimate , $\beta_{h,crit} \sim 2\%$. Thus the unstable mode is mainly driven by fluid term!

Outline

- Introduction to Energetic Particle (EP) Physics
- Hybrid model
- Quadratic form
- EP interaction with MHD modes
  - Internal kink mode/fishbone
  - Ballooning modes
  - Tearing mode
  - Resistive Wall Mode (RWM)
- Summary

Energetic Particle Stabilization of Ballooning Modes in Tokamaks

shown at least with respect to ballooning and internal kink modes.

The stabilizing effects of fast ions have been

Under these assumptions, we can investigate linear stability by means of the low-frequency kinetic energy principle[10,11] $\delta W = \delta W_f + \delta W_k$, where the fluid term is

$$\delta W_f = \tfrac{1}{2}\int (ds/B)\{\sigma|\nabla S|^2(\hat{b}\cdot\nabla\Phi)^2 + \tau[Q_\parallel - (\sigma/\tau)B\vec{e}\cdot\vec{\kappa}\Phi]^2 - (\vec{e}\cdot\vec{\kappa})[\vec{e}\cdot\tilde{\nabla}P_\parallel + (\sigma/\tau)\vec{e}\cdot\tilde{\nabla}P_\perp]\Phi^2\} \quad (1)$$

and the kinetic term (for the non-MHD energetic species) is

$$\delta W_k = \tfrac{1}{2}\int dE\, d\mu\, \vec{e}\cdot\nabla F_h \frac{[\int(ds/v_\parallel)(\mu Q_\parallel + v_\parallel{}^2\vec{e}\cdot\vec{\kappa}\Phi)]^2}{\int(ds/v_\parallel)(\mu\vec{e}\cdot\nabla B + v_\parallel{}^2\vec{e}\cdot\vec{\kappa})}. \quad (2)$$

Here, $Q_\parallel$ is the (Lagrangian) magnetic field perturbation parallel to the equilibrium field $\vec{B} = \hat{b}B$, and Φ is the perturbed electrostatic potential; $P_{\perp,\parallel}$ are the total pressure components; s is the arc length along a field line, and $\tilde{\nabla} = \nabla - (\nabla B)\partial/\partial B$, $\sigma = 1 + (P_\perp - P_\parallel)/B^2$, $\tau = 1 + (\partial P_\perp/B\partial B)$, $\vec{\kappa} = (\hat{b}\cdot\nabla)\hat{b}$, $\mu = v_\perp{}^2/2B$, and $E = v_\parallel{}^2/2 + \mu B$. We have restricted attention to high–mode-number interchange-ballooning modes, whose transverse variation is in the eikonal S, where $\hat{b}\cdot\nabla S = 0$ and $\vec{e} = \vec{B}\times\nabla S/B^2$. Equation (2) pertains to the high–bounce-frequency limit, appropriate for trapped fast particles, in which their distribution function F_h is constant on a field line. Hot particles trapped on the outside of a tokamak stabilize through δW_k, but are destabilizing in δW_f.

Rosenbluth, PRL 1983

Energetic Particle Stabilization of Ballooning Modes in Tokamaks

Rosenbluth, PRL 1983

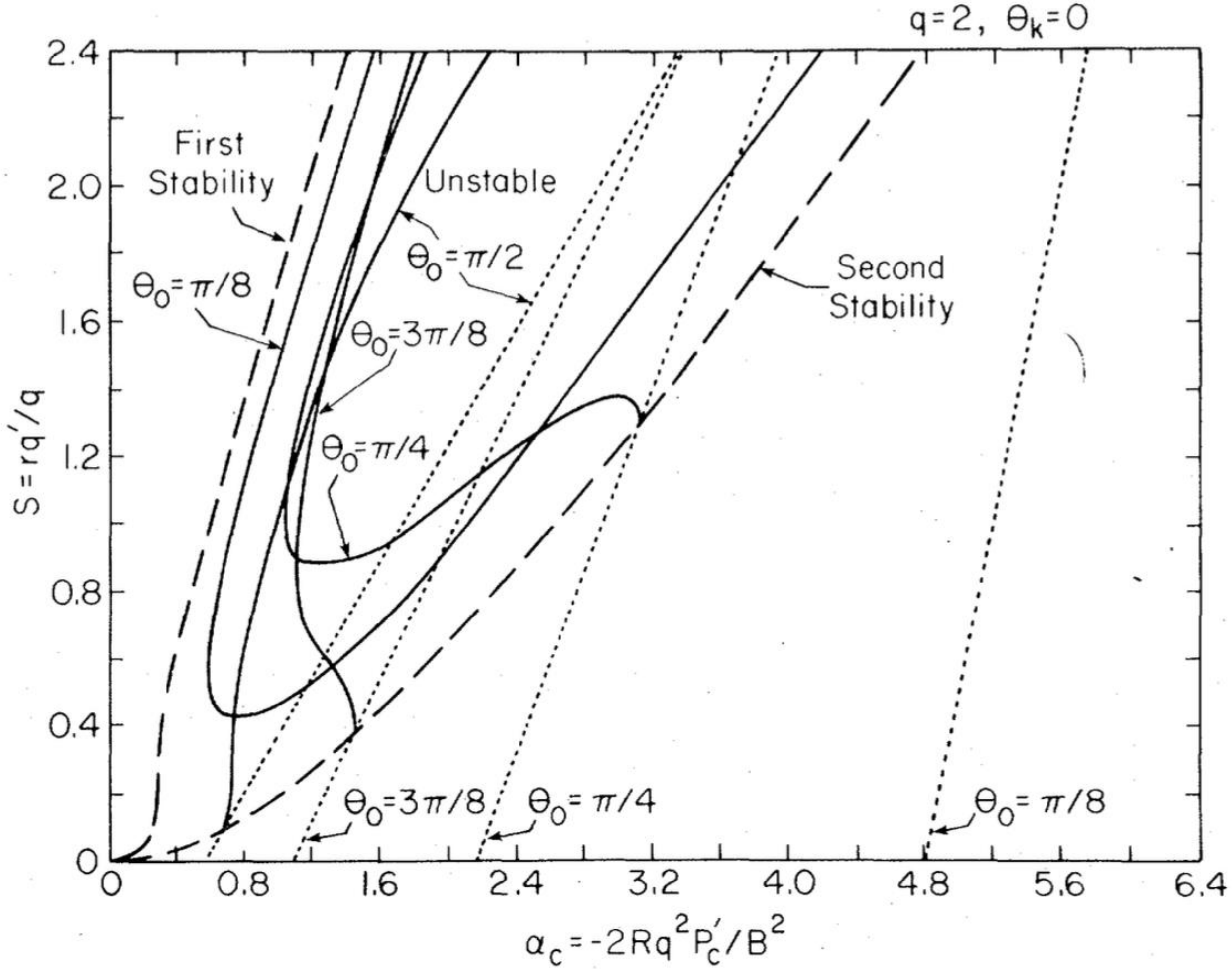

FIG. 1. Marginal stability boundaries in shear S and normalized core beta α_c, for maximal hot beta and various degrees of localization θ_0.

Outline

- Introduction to Energetic Particle (EP) Physics
- Hybrid model
- Quadratic form
- EP interaction with MHD modes
  - Internal kink mode/fishbone
  - Ballooning modes
  - Tearing mode
  - Resistive Wall Mode (RWM)
- Summary

M3D-K Simulation shows an unstable (2,1) tearing mode without EP for a model tokamak equilibrium

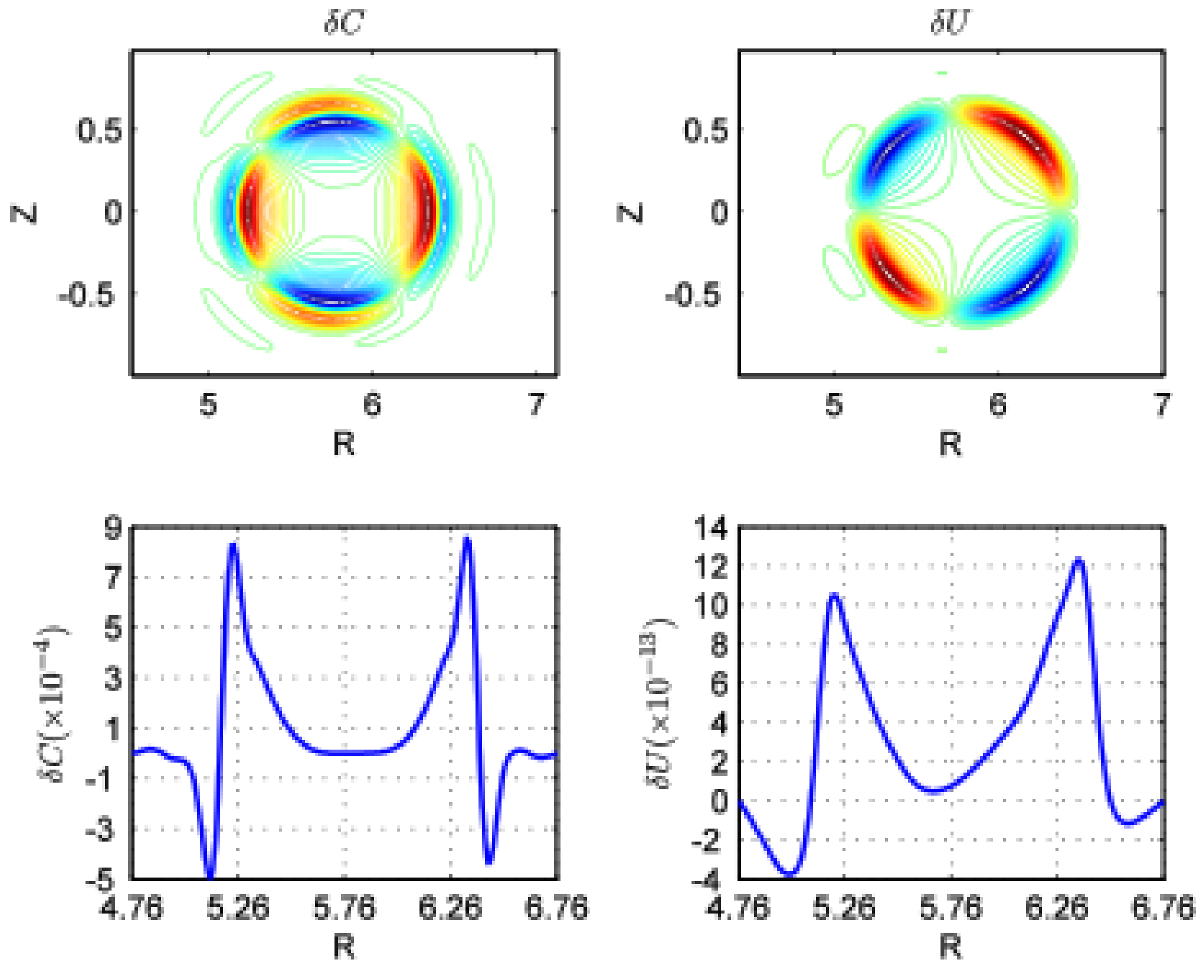

H.S. Cai and G.Y. Fu, Phys. Plasmas 2012

M3D-K simulation show the effects of co-passing/counter-passing energetic particles on tearing mode are stabilizing/destabilizing

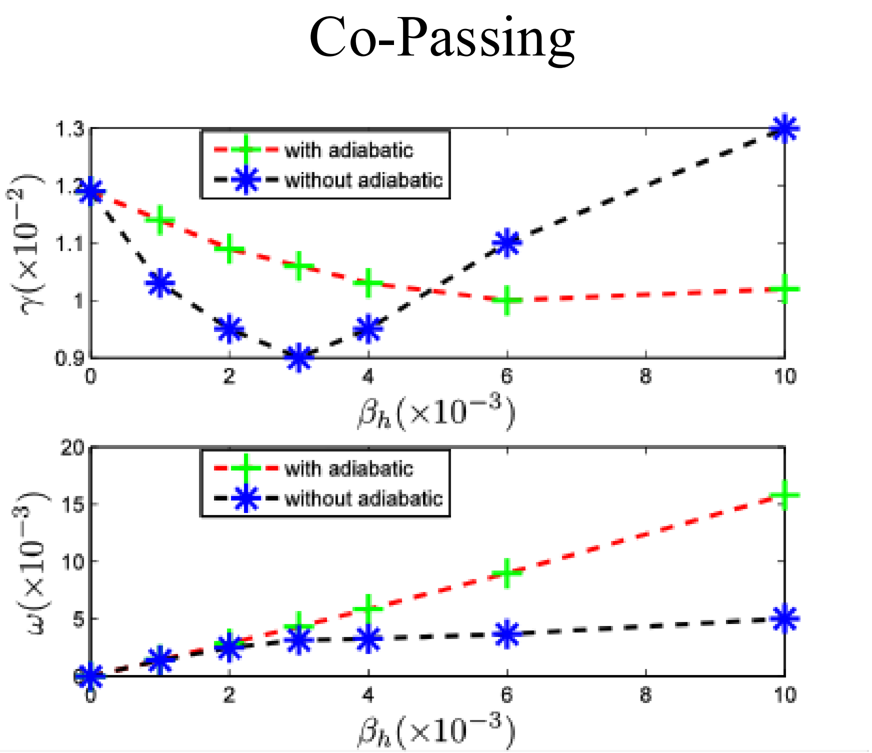

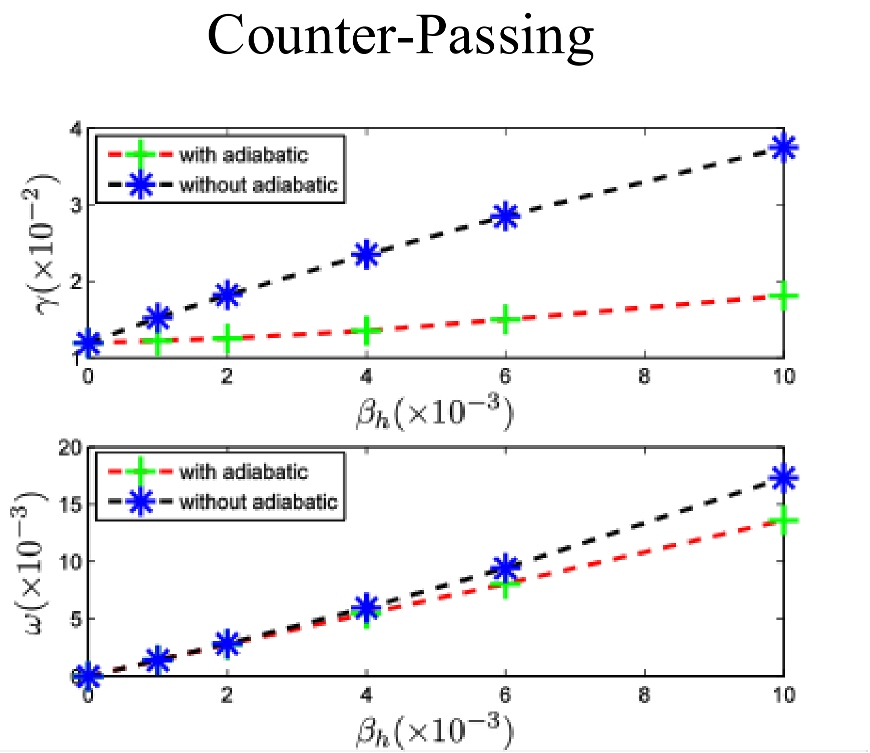

H.S. Cai and G.Y. Fu, Phys. Plasmas 2012

Outline

- Introduction to Energetic Particle (EP) Physics
- Hybrid model
- Quadratic form
- EP interaction with MHD modes
  - Internal kink mode/fishbone
  - Ballooning modes
  - Tearing mode
  - Resistive Wall Mode (RWM)
- Summary

Stabilization of the resistive wall mode instability by trapped energetic particles

$$D \equiv -i\omega\tau_w^* + \frac{\delta W^\infty + \delta W_{K0}}{\delta W^b + \delta W_{K0}} = 0,$$

$$\delta W_k = -2^{9/2}\pi^3 R m_h \int Brdr \int d\alpha \int dE E^{5/2} K_b \bar{J}^* \times \frac{Q}{\omega - \omega_0 - \omega_d} \bar{J},$$

Hao, PoP 2011

$$\delta W_{\mathrm{MHD},h} = -\int d^3x (\boldsymbol{\xi}_\perp \cdot \nabla P_{h\perp})(\boldsymbol{\xi}_\perp^* \cdot \boldsymbol{\kappa}),$$

Stabilization of the resistive wall mode instability by trapped energetic particles

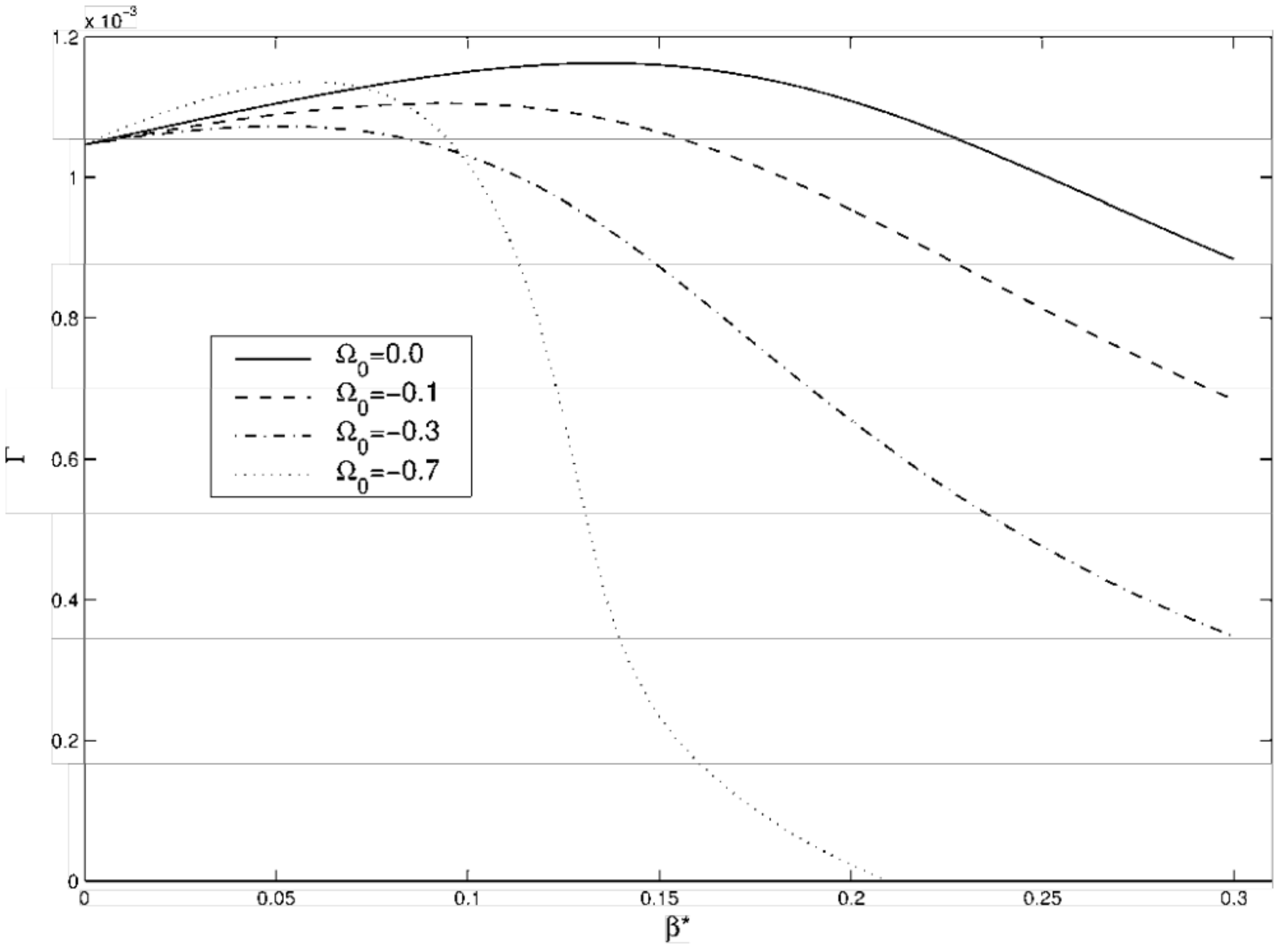

FIG. 6. The RWM normalized growth rate Γ as functions of the EPs beta β^* for various values of the plasma rotation frequency Ω_0. The wall position is taken as $b=1.2$.

Hao, PoP 2011

Energetic particle stabilization of RWM and excitation of fishbone-like mode

$$D = -i\omega\tau_w^* + \frac{\delta W^\infty + \delta W_k + \delta W_{\mathrm{MHD},h}}{\delta W^b + \delta W_k + \delta W_{\mathrm{MHD},h}} = 0,$$

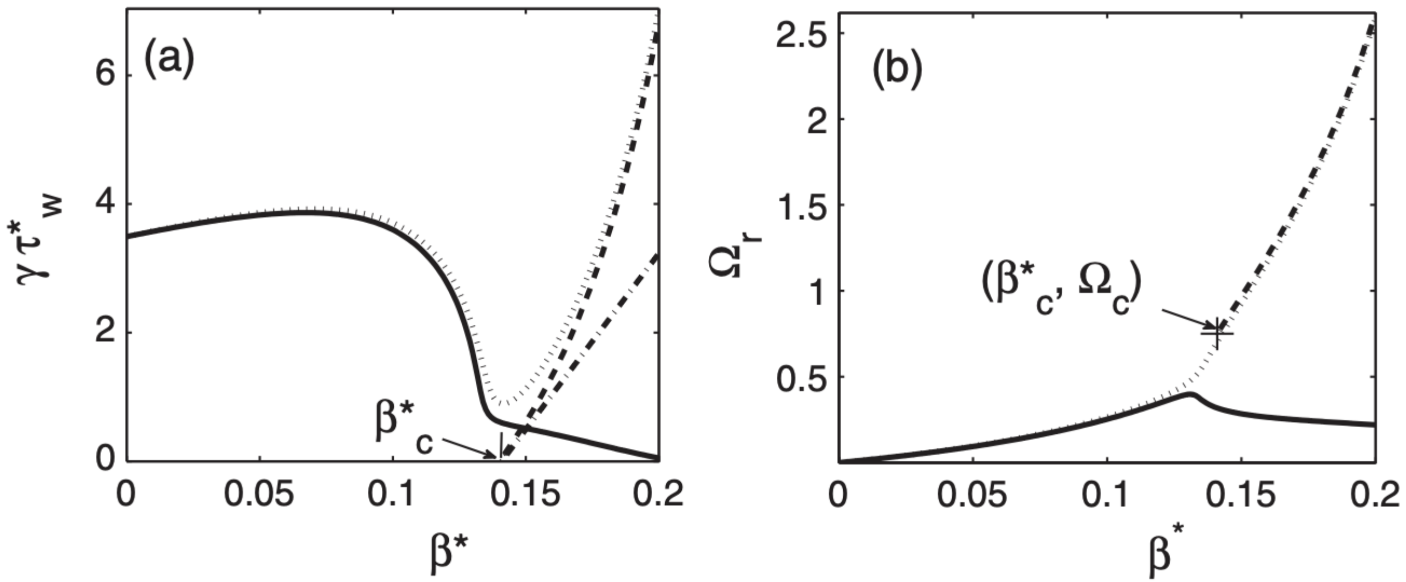

Hao, PRL 2011

FIG. 1. The (a) normalized growth rate $\gamma\tau_w^*$ and (b) mode frequency of the conventional RWM mode (solid curve) and the FLM (dashed curve) as functions of the trapped EPs' β^*, for the

Summary

- Kinetic response of energetic particles;
- Hybrid model
- Quadratic form;
- EP stabilization of internal kink and excitation of fishbone
- EP transport due to sawteeth, fishbone and NRK
- EP stabilization of ballooning modes
- EP effects on tearing modes;
- EP effects on RWM